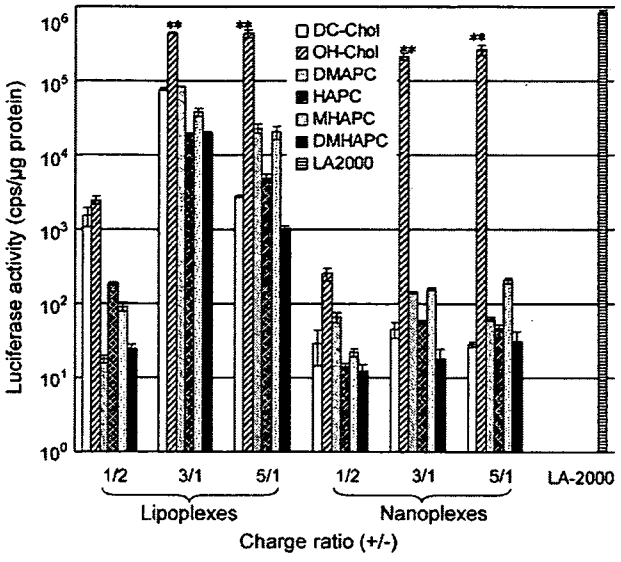

Fig. 4. Transfection efficiencies of lipoplexes and nanoplexes in A549 cells. The values were expressed as mean ± S.D. ($n = 3$). **Significant difference between OH-Chol and other CCDs in the same charge ratio group ($P < 0.01$, Student's t test). The values are expressed as mean ± S.D. ($n = 3$).

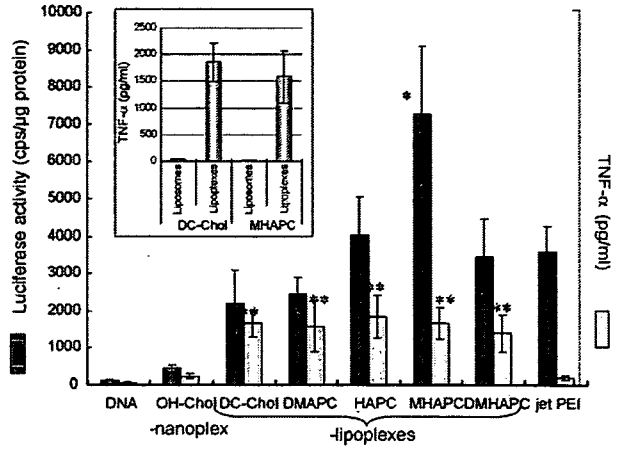

Fig. 5. Luciferase activity (closed columns) and TNF-α (open columns) in the lung at 24 h after intratracheal injection of lipoplexes and nanoplexes (+/− = 3/1). *Significant difference from OH-Chol nanoplex, jet-PEI, DC-Chol and DMHAPC lipoplexes ($P < 0.05$, Student's t test). **Significant difference from OH-Chol nanoplex and jet-PEI ($P < 0.01$, Student's t test). The values are expressed as mean ± S.D. ($n = 3$). The inset showed the TNF-α values of DC-Chol and MHAPC liposomes or lipoplexes in the lung at 24 h after intratracheal injection.

particle size from 150 to 300 nm at a charge ratio (+/−) of 3/1. The OH-Chol liposomes and nanoparticles formed large particles with DNA at charge ratios (+/−) of 3/1 and 5/1, and, therefore, for the *in vivo* study, we selected OH-Chol nanoplexes only at a charge ratio (+/−) of 3/1 as the optimum formulation.

3.3. Comparison between lipoplexes and nanoplexes for gene transfection in A549 cells

As shown in Fig. 4, the lipoplexes were far more effective than nanoplexes at the same charge ratio, especially at charge ratios (+/−) of 3/1 and 5/1. This may be explained by the contribution of the membrane destabilization role of DOPE in the liposomes. Among the six kinds of cationic cholesterol derivatives, OH-Chol lipoplexes and nanoplexes exhibited significantly elevated gene transfection, which may have been due to many factors, such as the amido linker and hydroxyethyl group in the structure of OH-Chol (Okayama et al., 1997), and some physical characteristics of the OH-Chol lipoplex and nanoplex, such as large particle size as shown in Fig. 3. The large particle size of OH-Chol lipoplex and nanoplex contributed partly to the high gene transfection in A549 cells, since large particles were more readily endocytosized into cells.

Furthermore, by comparing various lipoplexes at a charge ratio (+/−) of 3/1, we can see that the non-hydroxyethylated cationic cholesterol derivatives, DC-Chol and DMAPC, were more effective than hydroxyethylated ones (except for OH-Chol), namely DMHAPC, HAPC and MHAPC. Moreover, MHAPC, which bears a tertiary amine in the headgroup, exhibited a little higher transfection ability than HAPC and DMHAPC at the optimized formulation (CCD/DOPE = 1/2, molar ratio). Based on the higher gene transfection of lipoplexes than nanoplexes in A549 cells, we selected lipoplexes at a charge ratio (+/−) of 3/1 for further *in vivo* research.

3.4. Luciferase expression and TNF-α levels in the lung

Bolus intratracheal injection through the exposed bronchui of mouse was employed for all the *in vivo* studies. This administration method guarantees that 100% of the injected solution reaches the lung instantly (Driscoll et al., 2000). As long as the lipoplexes and nanoplexes can be stabilized under the mucus during distribution of the suspension in the lung, they have a chance to transfect the epithelial cells and even the alveolar cells in the lung.

As shown in Fig. 5, use of the lipoplexes resulted in much higher gene expression in the lung than use of OH-Chol nanoplexes, which were the most effective in A549 cells. One possible reason for this may be the insufficient DNA-protecting ability of OH-Chol nanoplexes in the presence of mucus and surfactants in the lung, while the lipoplexes might be able to encapsulate DNA in highly ordered multilammellar structures. Among these lipoplexes, DMHAPC, HAPC, and MHAPC lipoplexes, which were all hydroxyethylated in the cationic terminal, showed higher luciferase level than DC-Chol and DMAPC lipoplexes, which were not hydroxyethylated. In contrast to the *in vitro* data, the lipoplexes containing hydroxyethylated cationic cholesterol derivatives most strongly promoted gene expression in the lung. Although it is unclear how a hydroxyethyl group at the amine headgroup improves transfection, the hydroxyethyl moiety may affect the interaction between DNA and the cationic lipid membrane, and assist cellular association or some steps after internalization into the cells (Nakanishi and Noguchi, 2001).

Interestingly, the use of MHAPC lipoplexes, which contained a hydroxyethylated tertiary amine as the cationic part, resulted in 2- and 60-fold higher gene expression than the use of jet-PEI and naked DNA, respectively. The exact mechanism by which

Please cite this article in press as: Ding, W., et al., Hydroxyethylated cationic cholesterol derivatives in liposome vectors promote gene expression in the lung, Int J Pharm (2007), doi:10.1016/j.ijpharm.2007.10.051

the hydroxyethyl group in the cationic part and the tertiary amine in MHAPC increased gene expression is not known, but might be related to the stability of MHAPC lipoplexes in the presence of mucus and/or increased release of DNA from the lipoplexes in the acidic endosomal compartment.

Although the use of lipoplexes resulted in much higher gene expression in the lung, the lung seemed to have some inflammatory response to the lipoplex suspensions. The lipoplexes induced higher TNF-α secretion than OH-Chol nanoplexes and jet-PEI. The strong inflammatory response to lipoplexes was thought to be related to the lipoplexes themselves, since only low levels of TNF-α were detected with the DNA alone and DC-Chol and MHAPC liposomes alone (Fig. 5, inset). Furthermore, the high DOPE content in the lipoplexes might also have been responsible for the inflammatory response, since both OH-Chol nanoplexes and MHAPC nanoplexes induced low levels of TNF-α (data not shown). The present data were in accord with a report showing that lung toxicity observed with lipoplexes could be increased by the addition of DOPE, although DOPE suspension alone caused a negligible inflammatory response (Scheule et al., 1997).

3.5. Charge ratio of MHAPC lipoplex affected gene transfection

As shown in Fig. 3, the positively charged (+/− = 3/1) MHAPC lipoplexes were far more effective than negatively charged ones (+/− = 1/2) in A549 cells. Since most reports showed that nearly neutral or negatively charged lipoplexes/nanoplexes can produce higher gene expression in tumor tissues than positively charged ones (Miller, 2003; Hattori et al., 2007), we investigated the effect of the charge ratio (+/−) of MHAPC lipoplexes on gene transfection in the lung. In Fig. 6, it can be seen very clearly that the *in vivo* result corresponded to the *in vitro* one, with positively charged (+/− = 3/1) lipoplexes being significantly more effective than negatively charged ones. Since there are large amounts of surfactants and proteins in the lung lavage fluids and much mucin covers the epithelial cells in the lung, negatively charged lipoplexes might have a small chance of being retained as intact particles to transfect epithelial cells, whereas positively charged lipoplexes might be stable enough to exhibit gene expression ability (Rosenecker et al., 2003).

3.6. Distribution of MHAPC lipoplexes in the lung and localization of luciferase by immunostaining

Since MHAPC lipoplexes at a charge ratio (+/−) of 3/1 produced the highest gene expression in the lung, we investigated the distribution of rhodamine-labeled MHAPC lipoplexes and the location of the luciferase expression they produced after intratracheal injection. By observing the fluorescence of rhodamine in the cryosections, it was clear that rhodamine was mainly distributed throughout the bronchi and bronchioles, and some had even diffused to the alveolar cells (Fig. 7a and b). However, the distribution of lipoplexes was not homogeneous throughout the lungs: no fluorescence of rhodamine was observed in some other regions in the same slice (Fig. 7c and d). From the morphological observation of the lungs which received the MHAPC lipoplex suspension, only the upper and middle lobes exhibited an increased inflammatory response compared to normal lung tissue, indicating that the intratracheally injected lipoplex was mainly located in the upper and middle lobes (photos not shown).

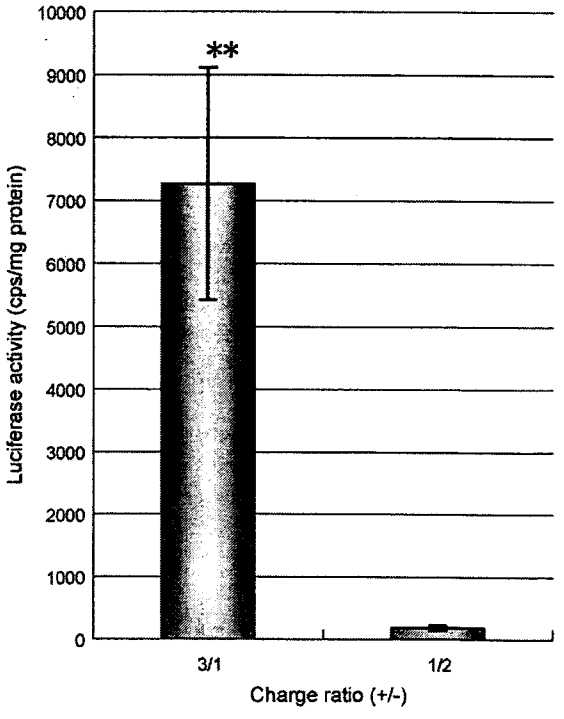

Fig. 6. Effect of charge ratio (+/−) of MHAPC lipoplexes on gene expression in the lung. **, Significant difference ($P < 0.01$, Student's t test). The values are expressed as mean ± S.D. ($n = 3$).

After luciferase immunostaining (Fig. 7e–h), the fluorescence of rhodamine was markedly decreased after many rounds of washing. The fluorescence was only located in the epithelial cells of the bronchi and bronchioles (Fig. 7f and h), and luciferase was also only expressed in the epithelial cells (Fig. 7e, arrows). Although some fluorescence of rhodamine was seen in the alveolar cells (Fig. 7b), there was no luciferase expression in the alveolar cells (Fig. 7e). We suppose that the fluorescence in the alveolar cells was mainly caused by free rhodamine-DHPE that became separated from the lipoplexes in the lung.

Lipoplexes administered by intravenous injection can be captured by the vascular system in the lung and induce gene expression in the lung alveolar region (Scheule et al., 1997). Since intratracheal injection has limited injection volume (1–2 ml/kg weight), the injected lipoplexes are directly exposed to the mucus around the bronchi and bronchioles, resulting in gene expression only in the epithelial cells lining the bronchi and bronchioles. This mode of injection, however, avoids gene expression in other organs, making it possible to decrease the dose of lipoplexes and possibly to decrease toxic side effects, and provides a potentially effective way for gene therapy of cystic fibrosis and other lung diseases.

Please cite this article in press as: Ding, W., et al., Hydroxyethylated cationic cholesterol derivatives in liposome vectors promote gene expression in the lung, Int J Pharm (2007), doi:10.1016/j.ijpharm.2007.10.051

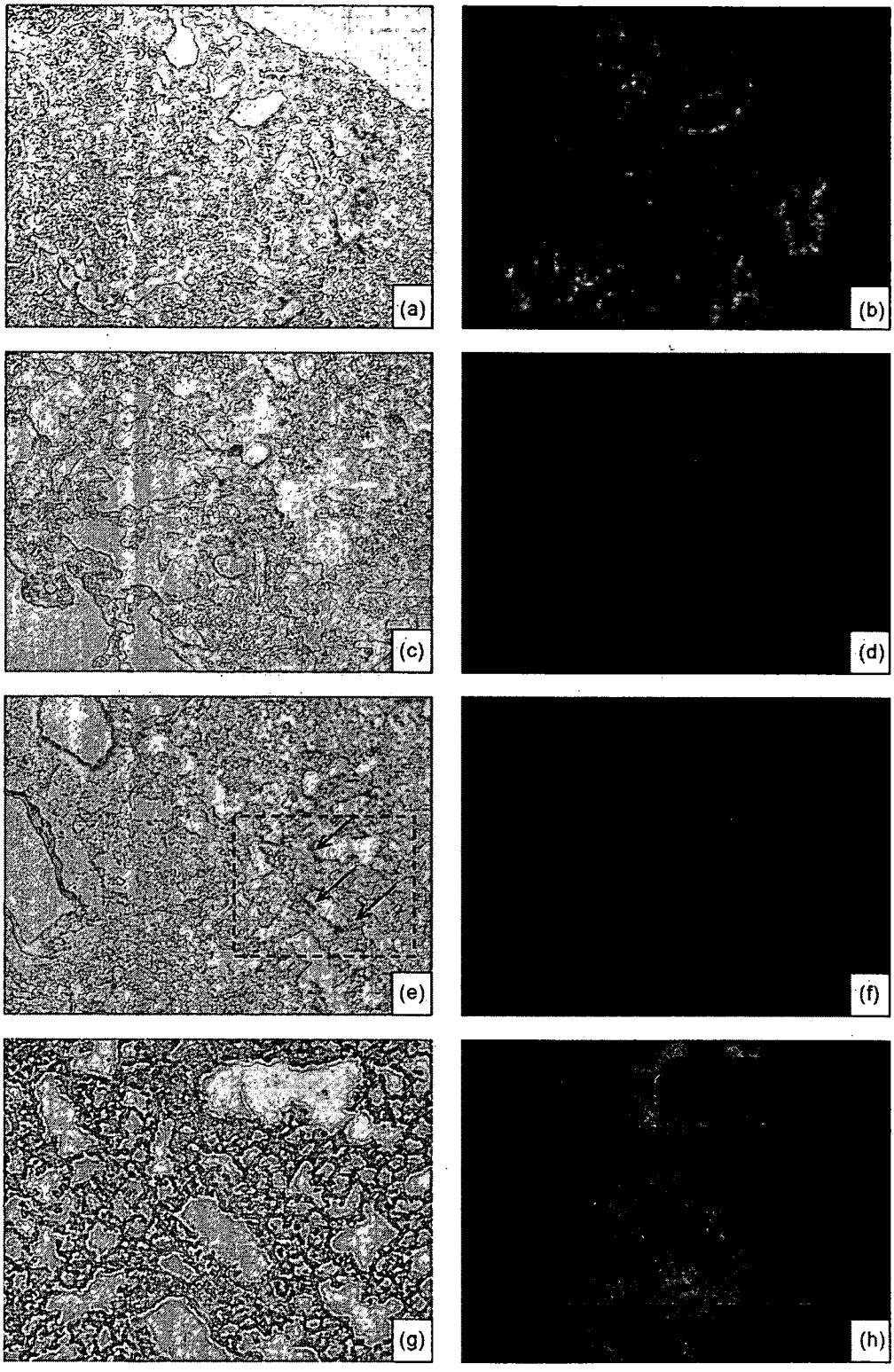

Fig. 7. Distribution of rhodamine-labeled MHAPC lipoplexes (a–d; before immunohistochemistry) and luciferase location in the lungs (e–h; after immunohistochemistry). a–f are shown at 40× magnification; g and h show 100× magnification of the regions in the dashed squares in e and f. Arrows in e indicate the luciferase (dark brown colored).

Please cite this article in press as: Ding, W., et al., Hydroxyethylated cationic cholesterol derivatives in liposome vectors promote gene expression in the lung, Int J Pharm (2007), doi:10.1016/j.ijpharm.2007.10.051

4. Conclusions

In the present work, three CCDs with a carbamate ester linker and a hydroxyethyl group were synthesized and formulated into liposomes and nanoparticles. In *in vitro* formulations, liposomes formulated with CCDs and DOPE of 1/2 molar ratio were more effective than the corresponding nanoparticles with CCDs and Tween 80 at all charge ratios. Furthermore, among the liposomal formulations, non-hydroxyethylated CCDs such as DC-Chol and DMAPC were more effective than hydroxyethylated ones in A549 cells. Gene transfection in the lung showed opposite results to those *in vitro*, with liposomes containing hydroxyethylated CCDs being more potent than ones containing non-hydroxyethylated CCDS. MHAPC liposomes, which contained a hydroxyethylated tertiary amine as the cationic part, showed the highest gene expression among CCD liposomes. All the lipoplexes caused higher TNF-α levels in the lung than the nanoplexes and jet-PEI and we considered the toxicity was largely caused by the lipoplex formulation, but our findings demonstrated that use of CCD lipoplexes with modification of the cationic cholesterol with a hydroxyethyl group at the tertiary amine headgroup, MHAPC, promoted gene expression in the lung without increasing the toxicity compared to other CCD lipoplexes. However, further efforts should be made to elucidate the mechanism of toxicity in the lung caused by CCD lipoplex and how to minimize the inflammation response of CCD lipoplex by optimizing the formulation.

Acknowledgements

This work was supported by a research grant of fiscal year 2006 from The Nagai Foundation, Tokyo and partially supported by the Ministry of Education, Culture, Sports, Sciences and Technology, Japan, and by the Open Research Center Project.

References

Arpicco, S., Canevari, S., Ceruti, M., Galmozzi, E., Rocco, F., Cattel, L., 2004. Synthesis, characterization and transfection activity of new saturated and unsaturated cationic lipids. Farmaco 59, 869–878.

Bajaj, A., Kondiah, P., Bhattacharya, S., 2007. Design, synthesis, and in vitro gene delivery efficacies of novel cholesterol-based Gemini cationic lipids and their serum compatibility: a structure–activity investigation. J. Med. Chem. 50, 2432–2442.

Choi, J.S., Lee, E.J., Jang, H.S., Park, J.S., 2001. New cationic liposomes for gene transfer into mammalian cells with high efficiency and low toxicity. Bioconjug. Chem. 12, 108–113.

Driscoll, K.E., Costa, D.L., Hatch, G., Henderson, R., Oberdorster, G., Salem, H., Schlesinger, R.B., 2000. Intratracheal instillation as an exposure technique for the evaluation of respiratory tract toxicity: uses and limitations. Toxicol. Sci. 55, 24–35.

Gao, X., Huang, L., 1991. A. novel cationic liposome reagent for efficient transfection of mammalian cells. Biochem. Biophys. Res. Commun. 179, 280–285.

Ghosh, Y.K., Visweswariah, S.S., Bhattacharya, S., 2002. Advantage of the ether linkage between the positive charge and the cholesteryl skeleton in cholesterol-based amphiphiles as vectors for gene delivery. Bioconjug. Chem. 13, 378–384.

Hasegawa, S., Hirashima, N., Nakanishi, M., 2002. Comparative study of transfection efficiency of cationic cholesterols mediated by liposomes-based gene delivery. Bioorg. Med. Chem. Lett. 12, 1299–1302.

Hattori, Y., Kubo, H., Higashiyama, K., Maitani, Y., 2005. Folate-linked nanoparticles formed with DNA complexes in sodium chloride solution enhance transfection efficiency. J. Biomed. Nanotechnol. 1, 176–184.

Hattori, Y., Ding, W., Maitani, Y., 2007. Highly efficient cationic hydroxyethylated cholesterol-based nanoparticle-mediated gene transfer in vivo and in vitro in prostate carcinoma PC-3 cells. J. Control. 120, 122–132.

Hoag, H., 2005. Gene therapy rising? Nature 435, 530–531.

Igarashi, S., Hattori, Y., Maitani, Y., 2006. Biosurfactant MEL-A enhances cellular association and gene transfection by cationic liposome. J. Control. Release 112, 362–368.

Lee, E.J., Lee, M., Park, J.S., Choi, J.S., 2006. Synthesis of 3β [L-lysinamidecarbamoyl] cholesterol derivatives by solid-phase method and characteristics of complexes with antisense oligodeoxynucleotides. Bull. Korean Chem. Soc. 27, 1020–1024.

Maitani, Y., Igarashi, S., Sato, M., Hattori, Y., 2007. Cationic liposome (DC-Chol/DOPE = 1:2) and a modified ethanol injection method to prepare liposomes, increased gene expression. Int. J. Pharm..

Miller, A.D., 2003. The problem with cationic liposome/micelle-based non-viral vector systems for gene therapy. Curr. Med. Chem. 10, 1195–1211.

Nakanishi, M., 2003. New strategy in gene transfection by cationic transfection lipids with a cationic cholesterol. Curr. Med. Chem. 10, 1289–1296.

Nakanishi, M., Noguchi, A., 2001. Confocal and probe microscopy to study gene transfection mediated by cationic liposomes with a cationic cholesterol derivative. Adv. Drug Deliv. Rev. 52, 197–207.

Okayama, R., Noji, M., Nakanishi, M., 1997. Cationic cholesterol with a hydroxyethylamino head group promotes significantly liposome-mediated gene transfection. FEBS Lett. 408, 232–234.

Percot, A., Briane, D., Coudert, R., Reynier, P., Bouchemal, N., Lievre, N., Hantz, E., Salzmann, J.L., Cao, A., 2004. A hydroxyethylated cholesterol-based cationic lipid for DNA delivery: effect of conditioning. Int. J. Pharm. 278, 143–163.

Pietersz, G.A., Tang, C.K., Apostolopoulos, V., 2006. Structure and design of polycationic carriers for gene delivery. Mini Rev. Med. Chem. 6, 1285–1298.

Reynier, P., Briane, D., Coudert, R., Fadda, G., Bouchemal, N., Bissieres, P., Taillandier, E., Cao, A., 2004. Modifications in the head group and in the spacer of cholesterol-based cationic lipids promote transfection in melanoma B16–F10 cells and tumours. J. Drug Target. 12, 25–38.

Rosenecker, J., Naundorf, S., Gersting, S.W., Hauck, R.W., Gessner, A., Nicklaus, P., Müller, R.H., Rudolph, C., 2003. Interaction of bronchoalveolar lavage fluid with polyplexes and lipoplexes: analysing the role of proteins and glycoproteins. J. Gene Med. 5, 49–60.

Scheule, R.K., St George, J.A., Bagley, R.G., Marshall, J., Kaplan, J.M., Akita, G.Y., Wang, K.X., Lee, E.R., Harris, D.J., Jiang, C., Yew, N.S., Smith, A.E., Cheng, S.H., 1997. Basis of pulmonary toxicity associated with cationic lipid-mediated gene transfer to the mammalian lung. Hum. Gene Ther. 8, 689–707.

Venkata Srilakshmi, G., Sen, J., Chaudhuri, A., Ramadas, Y., Madhusudhana Rao, N., 2002. Anchor-dependent lipofection with non-glycerol based cytofectins containing single 2-hydroxyethyl head groups. Biochim. Biophys. Acta 1559, 87–95.

Please cite this article in press as: Ding, W., et al., Hydroxyethylated cationic cholesterol derivatives in liposome vectors promote gene expression in the lung, Int J Pharm (2007), doi:10.1016/j.ijpharm.2007.10.051

THE JOURNAL OF GENE MEDICINE
J Gene Med 2007; 9: 976–985.
Published online 17 September 2007 in Wiley InterScience (www.interscience.wiley.com) DOI: 10.1002/jgm.1104

RESEARCH ARTICLE

Adiponectin gene therapy of streptozotocin-induced diabetic mice using hydrodynamic injection

Masayoshi Fukushima[1]
Yoshiyuki Hattori[1]
Hideo Tsukada[2]
Kimiko Koga[1]
Eiichi Kajiwara[1]
Kumi Kawano[1]
Tsuneo Kobayashi[1]
Katsuo Kamata[1]
Yoshie Maitani[1]*

[1]*Institute of Medicinal Chemistry, Hoshi University, Shinagawa-ku, Tokyo 142-8501, Japan*

[2]*Central Research Laboratory, Hamamatsu Photonics, Hamamatsu, Shizuoka 434-8601, Japan*

*Correspondence to: Yoshie Maitani, Institute of Medicinal Chemistry, Hoshi University, Shinagawa-ku, Tokyo 142-8501, Japan.
E-mail: yoshie@hoshi.ac.jp

Received: 9 April 2007
Revised: 3 August 2007
Accepted: 8 August 2007

Abstract

Background Adiponectin (Adipo), an adipocyte hormone involved in the regulation of glucose and lipid metabolism, has already been identified as a potential therapeutic target for the treatment of diabetes. However, successful delivery of Adipo to the receptors is difficult due to their peptide characteristics. Receptors for Adipo are abundantly expressed in the liver and skeletal muscle.

Methods Uptake of 2-(*N*-(7-nitrobenz-2-oxa-1,3-diazol-4-yl)amino)-2-deoxyglucose (2-NBDG) in hepatoblastoma HepG2 cells expressing Adipo was examined. Adipo-expressing plasmid DNA (10–50 μg) in saline solution (0.1 ml/g body weight) was rapidly injected into the tail vein of 4-week-old diabetic mice after 4–6 weeks of treatment with streptozotocin (STZ). Uptake of glucose in diabetic mice also was measured using a planar positron imaging system featuring 18-fluorodeoxyglucose.

Results HepG2 cells expressing Adipo exhibited significantly increased 2-NBDG uptake compared with cells transfected with control plasmid even in the absence of insulin. STZ-induced diabetic mice showed decreased serum Adipo levels compared with non-diabetic mice. A single hydrodynamic injection of 10–50 μg Adipo-expressing plasmid DNA into diabetic mice led to approximately 10-15-fold elevation in serum Adipo levels, and resulted in decreased serum levels of glucose and triglyceride. As well as exhibiting higher levels of Adipo expression, diabetic mice also had higher hepatic glucose uptake than similar mice injected with control plasmid.

Conclusions We report that STZ-induced diabetic mice exhibited decreased Adipo levels and hyperglycemia which may be alleviated by hydrodynamic injection of the Adipo gene. This type of gene delivery system to the liver offers a different approach in developing novel treatments for type 1 and 2 diabetes. Copyright © 2007 John Wiley & Sons, Ltd.

Keywords adiponectin; gene expression; glucose-lowering effect; STZ-induced diabetic mice; glucose uptake; receptor targeting

Introduction

Adiponectin (Adipo) is an adipocyte hormone involved in glucose and lipid metabolism [1–4]. Impaired glucose and lipid metabolism, hallmarks of obesity and type 2 diabetes [5], promote excessive lipid storage in insulin target tissues, such as muscle and the liver, thereby leading to insulin

resistance [6]. Cell-surface receptors of Adipo (AdipoR1 and AdipoR2) have been cloned [7] and their expression patterns revealed: AdipoR1 was abundantly expressed in skeletal muscle, whereas AdipoR2 was principally expressed in the liver [7]. The insulin-sensitizing effects of Adipo in insulin-resistant mice correlated with an increase in the activity of AMPK (5′-AMP-activated protein kinase), which could be directly related to the binding of Adipo to AdipoR1 and AdipoR2.

Adipo has already been identified as a potential therapeutic target for the treatment of diabetes and other obesity-related illnesses [8]. However, successful delivery of Adipo to these receptors is difficult due to their peptide characteristics. Use of adeno-associated virus vectors to mediate Adipo expression led to an improvement in insulin sensitivity in diet-induced obese rats [9] compared to non-obese rats [10], and this was due to an increase in AMPK activity as well as modulation of hepatic gluconeogenesis [10]. Recent advances in gene therapy have already targeted receptors. The hydrodynamic injection method can provide a route for efficient hepatic expression of transgenes in mice just by systemic administration of naked DNA [11–14]. However, to our knowledge, hydrodynamic injections of Adipo genes targeted to liver have not yet been reported. Therefore, we used this method to evaluate the usefulness of Adipo gene therapy to the liver for diabetes.

The effects of Adipo on mice with type 2 diabetes have been extensively studied [8,15], but the effects of Adipo on mice with type 1 diabetes are less clear. Therefore, at first we investigated Adipo levels in streptozotocin (STZ)-induced diabetic mice. We aimed to induce transfection of full-length Adipo plasmid DNA (pCMV-Ad) in liver, via hydrodynamic injection since full-length Adipo protein has a higher binding affinity to hepatic membrane fractions than globular Adipo [16].

We found that STZ-induced diabetic mice showed decreased Adipo levels, and that the gene delivery of pCMV-Ad in STZ-induced diabetic mice via hydrodynamic injection significantly increased serum and hepatic concentrations of Adipo, and decreased serum glucose and triglyceride levels in these mice. This glucose-lowering effect was likely to be directly related to an increase in glucose uptake in the liver.

Materials and methods

Cell culture

Human hepatoblastoma (HepG2) cells were obtained from the Riken Cell Bank (Ibaraki, Japan) and were grown in RPMI-1640 medium supplemented with 10% heat-inactivated serum.

Plasmid constructions

Complementary DNA was synthesized from the total RNA in mouse adipose tissue (Biochain Institute, CA, USA). In the construction of pCMV-Ad, cDNA coding for bp 1–744 of mouse Adipo was amplified by polymerase chain reaction (PCR) using the following Adipo-specific primers: Adipo forward primer (5′-GAAAAGCTTaccATGCTACTGTTGCAAGCTCTC); Adipo reverse primer (5′-GAATCTAGATCAGTTGGTATCATGGTAGA). The forward primer contained a 3-bp optimal Kozak sequence (in lower-case letters) together with a *Hind* III restriction site (underlined). The reverse primer coding for bp 723–744 of Adipo had an *Xba* I restriction site (underlined). Cytomegalovirus (CMV) promoter DNA was amplified and digested with *Kpn* I and *Hind* III as previously reported [17]. After amplification, Adipo cDNA was digested with *Hind* III and *Xba* I, and ligated into a *Hind* III/*Xba* I-digested pGL3-enhancer (Promega, Madison, WI, USA). The plasmid was then digested with *Kpn* I and *Hind* III, and ligated with CMV promoter DNA [17]. In the construction of the plasmid pCMV-luc encoding luciferase gene, pGL3 enhancer was digested with *Kpn* I and *Hind* III, and was ligated with the CMV promoter. pGL3-basic encoding the luciferase gene without a promoter was obtained from Promega, and used as a control plasmid. A protein-free preparation of the plasmid was purified after alkaline lysis in Maxiprep columns (Qiagen, Hilden, Germany) without contamination with LPS (less than 0.1 EU/1 μg plasmid DNA).

Adipo expression and AMPK activity

HepG2 cells were cultured on 35-mm dishes. These cells were transfected with 2 μg of pCMV-Ad, or pGL3-basic as a control, using Lipofectamine 2000 (Invitrogen Corp., Carlsbad, CA, USA), and then incubated for 24 h. To reveal AMPK activation, the cells were treated with 1 mM 5-aminoimidazole-4-carboxamide-1-D-riboside (AICAR) (Wako, Osaka, Japan) for 0, 10, 30, 60 or 180 min. Cell protein extracts were prepared with 1 ml of sampling buffer containing 1% (v/v) Triton X-100, protease inhibitor cocktail set III and protein tyrosine phosphatase inhibitor II (Calbiochem, Darmstadt, Germany) in phosphate-buffered saline (PBS). They were separated by 7.5 or 12.5% (w/v) sodium dodcecyl sulfate polyacrylamide gel electrophoresis (SDS-PAGE) and then transferred onto polyvinylidene difluoride membranes (Nippon Genetics, Tokyo, Japan). Membranes were blocked at room temperature for 1 h with PBS containing 0.1% (v/v) Tween-20 and 5% (w/v) skimmed milk, and subsequently incubated at room temperature for 1 h with rabbit anti-mouse adiponectin polyclonal antibody (Assay pro, MO, USA) or rabbit anti-phospho-AMPK-α (Thr-172) monoclonal antibody (Cell Signaling Technology, MA, USA). Membranes were then incubated with a horseradish peroxidase-conjugated, goat, anti-rabbit, IgG antibody (Santa Cruz Biotechnology, CA, USA) as a secondary antibody. To enhance the antibody signal, all antibodies were diluted with Can Get Signal (Toyobo, Osaka, Japan). The signal was

detected using a SuperSignal West Pico chemiluminescent substrate (Pierce, Rockford, IL, USA). Mouse Adipo levels in cells and culture media were determined by Mouse/Rat adiponectin enzyme-linked immunosorbent assay (ELISA) kit (Otsuka Pharmaceutical Co., Ltd., Tokushima, Japan).

2-(*N*-(7-Nitrobenz-2-oxa-1,3-diazol-4-yl)amino)-2-deoxyglucose (2-NBDG) uptake

HepG2 cells were cultured on 96-well black cell culture dishes. In AICAR experiments, cells were incubated with 1 mM AICAR for 60 min. In transfection experiments, cells were incubated for 24 h after transfection of pGL3-basic or pCMV-Ad using Lipofectamine 2000. After AICAR treatment or DNA transfection, all cells were incubated with 50 μM 2-NBDG (Molecular Probes, OR, USA) in PBS for 15 min, and then washed with additional PBS to remove excess 2-NBDG. Fluorescence in the cells was measured at an excitation wavelength of 485 nm and an emission wavelength of 535 nm with a Wallac ARVO SX 1420 multi-label counter (Perkin Elmer Life Sciences, Japan, Co. Ltd., Kanagawa, Japan).

Animal studies

Male ICR mice (aged 4 weeks, Tokyo Laboratory Animal Science, Co., Ltd., Tokyo, Japan) were used in this study. The mice were maintained in accordance with institutional guidelines of the Hoshi University Animal Care and Use committee. Each mouse received an intravenous injection of 200 mg/kg STZ to induce diabetes [18]. Mice were fasted for 3 h before commencing the experiment and prior to taking blood samples. Glucose concentration of each sample was measured using Medisafe Mini (Terumo, Tokyo, Japan). Mice with blood glucose levels over 500 mg/dl and 20–30g body weight were selected for testing 4 to 6 weeks after STZ treatment. To transfect pCMV-Ad into mice, we used a hydrodynamic injection method: Injection into the tail vein in 5 s with 2.5 ml of saline solution containing 1, 5, 10 or 50 μg of pCMV-luc, pGL3-basic or pCMV-Ad [11,12]. Serum concentrations of insulin, glucagon and triglyceride (TG) were measured using an Ibis insulin ELISA kit (Sibayagi, Gunma, Japan), a glucagon EIA kit (Yauchihara, Shizuoka, Japan) and a triglyceride E test (Wako, Osaka, Japan), respectively. Serum Adipo levels were measured by ELISA, as described above. Twenty-four hours after plasmid injection, mice were anesthetized and perfused with saline through the left ventricle, and those that had received pGL3-basic or pCMV-Ad were sacrificed. Liver and skeletal muscle were harvested, homogenized with sampling buffer and centrifuged at 15 000 *g*. Supernatant fractions were subjected to Western blot analysis to detect expression of Adipo and phosphor-AMPK-α, and the concentration of Adipo was measured using the above method.

Distribution of 18-fluorodeoxyglucose (FDG) using a planar positron imaging system

An anesthetized mouse, which had been fasting for at least 12 h, was fixed onto the stage plate [19,20]. FDG, a short-lived glucose analogue labeled with fluorine-18 ($t_{1/2}$ = 110 min) (4 MBq/20 g), was injected intravenously into the STZ-induced diabetic mouse through the tail vein 18 to 24 h after hydrodynamic injection of 10 μg of pGL3-basic or pCMV-Ad. After FDG injection, image data were acquired at 1-min frame intervals for 60 min with a PPIS-4800 planar positron imaging system (Hamamatsu Photonics, Hamamatsu, Japan). The distribution and kinetics of FDG *in vivo* were analyzed from a composite image accumulated during the last 20 min of data acquisition. The region of interest (ROI) was preset on the composite image, and the time-activity curves of radioactivity in the heart, liver and muscle tissues were monitored for 60 min after FDG injection.

Adipo receptor mRNA expression in the liver

Total liver RNA was isolated using the Quickprep Total RNA extraction kit (Amersham Biosciences, NJ, USA) 24 h after hydrodynamic injection of pGL3-basic or pCMV-Ad. UV spectrometry measurements at 260 nm and 280 nm were used to assess RNA yield, and RNA purity was analyzed by electrophoresis. Complementary DNA was synthesized from the total amount of RNA extracted from the liver, real-time PCR was performed with the iCycler MyiQ detection system (Bio-Rad Laboratories, Hercules, CA, USA), and a SYBR Green I assay (iQ™ SYBER Green Supermix, Bio-Rad Laboratories) was used for quantification. PCR amplification required denaturation at 94 °C for 0.5 min, primer annealing at 58 °C for 0.5 min, and elongation at 72 °C for 1 min for 40 cycles. PCR amplification of the housekeeping gene β-actin, and AdipoR1 and AdipoR2 mouse Adipo receptors, were performed within the same cycle for all samples. For the amplification of mouse AdipoR1, the primers AdipoR1-FW, 5′-TGATGTGCTTCCTGACTGGCTGAAAGAC-3′, and AdipoR1-RW, 5′-TCAAGCCAAGTCCCAGGAACACTCCT-GC-3′, were used. For the amplification of mouse AdipoR2, the primers AdipoR2-FW, 5′-CGAATGGAAGAGTTTGTTT-GTAAGGTGT-3′, and AdipoR2-RW, 5′-GATTCCACTCAG-GCCTAAGCCCACGAAC-3′, were used. For the amplification of mouse β-actin, the primers β-actin-FW, 5′-ACCCACACTGTGCCCATCTA-3′, and β-actin-RW, 5′-CTGCTTGCTGATCCACATCT-3′, were used. Samples were analyzed in triplicate and the expression level of Adipo receptor mRNA was normalized for the amount of β-actin in the same sample. A difference of one cycle was calculated to be the equivalent of a 2-fold change in gene expression.

Statistical analysis

Significant differences in mean values were evaluated using Student's unpaired *t*-test. A *P*-value of less than 0.05 was considered to be significant.

Results

Adipo gene transfection in HepG2 cell cultures

ELISA analysis was used to quantify Adipo levels in HepG2 cells transfected with pCMV-Ad, and its surrounding culture medium. High levels of Adipo protein were detected in cells that had been transfected with pCMV-Ad, whereas Adipo protein was not detected at all in both non-transfected and pGL3-basic-transfected cells (Figure 1). Samples taken 24 h post-transfection showed Adipo levels to be 183 ± 30 ng/ml in HepG2 cells and 107 ± 25 ng/ml in the culture medium when measured by ELISA (Figure 1).

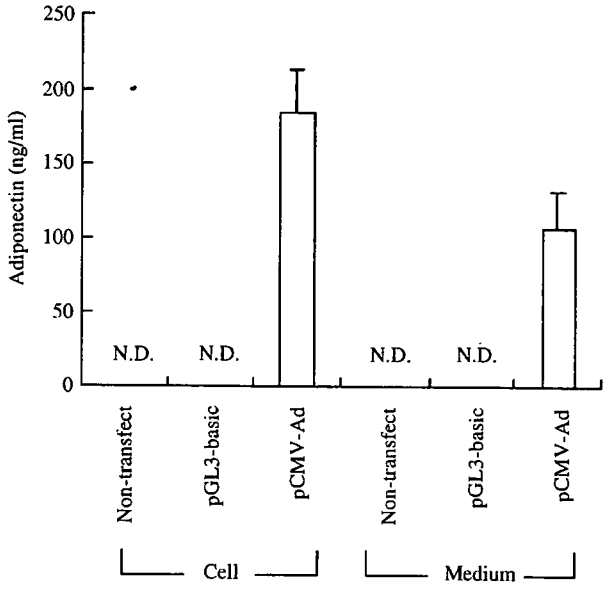

Figure 1. Adipo expression in HepG2 cells transfected with pCMV-Ad. Adipo levels in HepG2 cells and culture medium 24 h after transfection with pCMV-Ad were determined by ELISA; n = 3 for each sample. Each bar represents the mean ± standard deviation (S.D.) N.D.: not detected

Adipo stimulates the phosphorylation of AMPK and glucose uptake in HepG2 cells

Yamauchi *et al.* reported that Adipo activity requires liver AMPK activation in mice [16]. To investigate Adipo activity in pCMV-Ad-transfected HepG2 cells, the level of AMPK activation was studied. Cell phosphorylation of AMPK (p-AMPK) was measured using Western blot analysis. As a control, HepG2 cells were treated with AICAR, a cell-permeable activator of AMPK, which sustained the phosphorylation of Thr 172 in the α-subunit of AMPK (α-AMPK) in proportion to the incubation time (Figure 2a). Cells transfected with pCMV-Ad also exhibited an increase in p-AMPK (Figure 2b).

Next, to investigate glucose uptake by AMPK activation, uptake of 2-NBDG, a metabolizable fluorescent derivative of glucose, in HepG2 cells treated with AICAR or transfected with pGL3-basic or pCMV-Ad was measured. There was no increase in cellular uptake of 2-NBDG 1 h after treatment with 1 mM AICAR, but the level of uptake in cells transfected with pCMV-Ad had significantly increased compared with cells transfected with pGL3-basic (Figure 2c).

Reduction of Adipo levels in STZ-induced diabetic mice

Prior to transfection, time-dependent changes in serum Adipo levels in non-diabetic and STZ-induced diabetic mice were investigated for 4–6 weeks. As a murine model of type 1 diabetes, serum Adipo levels in diabetic mice declined within 2 weeks of STZ treatment and continued for a further 5 weeks, exhibiting overall lower serum Adipo levels than non-diabetic mice (Figure 3a). This effect appeared 4–6 weeks after the treatment with STZ in mice aged 4 weeks, despite persistently high serum glucose levels (Figure 3b). Serum Adipo levels in non-diabetic mice were 15.0 ± 2.08 µg/ml, while those in STZ-induced diabetic mice 4–6 weeks after STZ treatment were 7.10 ± 1.88 µg/ml (Figure 3c). The concentration of serum glucose in non-diabetic mice was in the range of 150 to 200 mg/dl, while those of STZ-induced diabetic mice were over 500 mg/dl 1 week after STZ treatment (Figure 3b). Average serum concentration of insulin in non-diabetic mice was 2.60 ± 0.37 ng/ml, but the presence of insulin was not detected at all in serum samples from STZ-induced diabetic mice 4–6 weeks after treatment with STZ (Figure 3d).

Expression of Adipo in STZ-induced diabetic mice

To confirm gene expression had occurred in the liver post-hydrodynamic injection, plasmid DNA encoding luciferase (pCMV-luc) was administered by the same method into STZ-induced diabetic mice and non-diabetic control mice. Twenty-four hours post-injection, mice from both cohorts were sacrificed, and luciferase activity in the liver, kidneys, lungs, and spleen was measured. Luciferase activity in the liver was 100–1000-fold higher than the kidneys, lungs or spleen, but was not detected in the muscle in both non-diabetic and STZ-induced diabetic mice (data not shown). This result correlated with published data and indicated that hydrodynamic injection was an effective method for gene delivery to the liver [11,12].

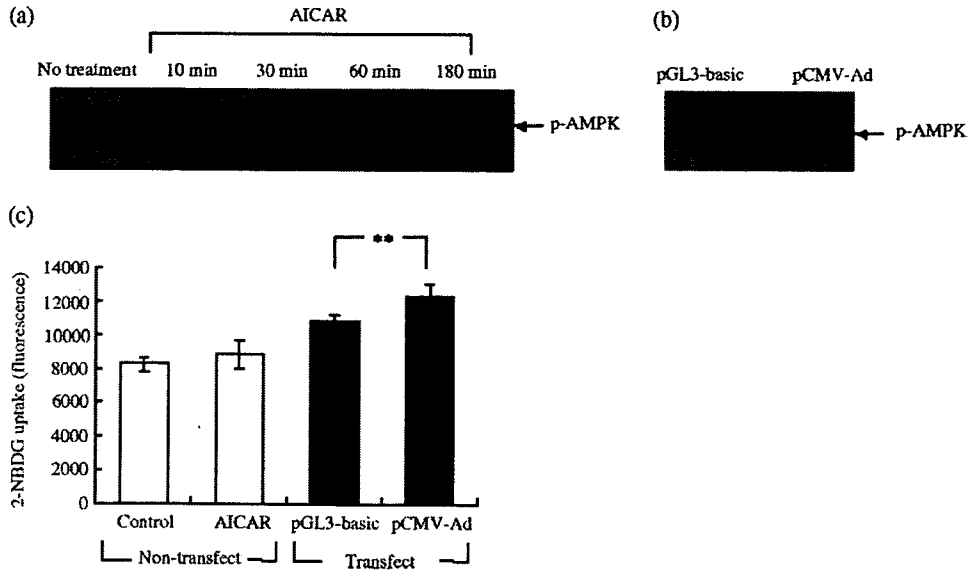

Figure 2. Western blot analysis showing increased AMPK activity in HepG2 cells treated with AICAR (a) or transfected with pCMV-Ad (a, b), and cells transfected with pCMV-Ad showing 2-NBDG uptake (c). (a) Phosphorylation of AMPK in HepG2 cells treated with 1 mM AICAR for 0, 10, 30, 60 and 180 min. (b) Phosphorylation of AMPK in HepG2 cells 24 h after transfection with 10 μg of pGL3-basic or pCMV-Ad. (c) Cellular uptake of 2-NBDG for 15 min after 1 h treatment with 1 mM AICAR, or after 24 h transfection with either pGL3-basic or pCMV-Ad. Each bar represents the mean ± S.D.; $n = 4$. $^{**}P < 0.01$; compared with pGL3-basic

The relationship between dose dependency and Adipo expression of plasmid DNA in STZ-induced diabetic mice was examined by administering hydrodynamic injections of pGL3-basic as control plasmid DNA, with 1, 5, 10 or 50 μg of pCMV-Ad. Results showed that the transfection of pGL3-basic and 1 μg of pCMV-Ad did not affect serum Adipo levels in STZ-induced diabetic mice, but transfection of 5 μg or 10 μg of pCMV-Ad significantly raised serum Adipo levels approximately 4-fold and 15-fold, respectively, 24 h after injection, when compared with pre-injection measurements (Figure 4a). Elevated Adipo levels were sustained up to the 48-h mark, before declining gradually during the 48–72-h post-injection interval (Figure 4a). Administration of 50 μg of pCMV-Ad induced slightly higher serum Adipo levels than that of 10 μg of pCMV-Ad at the 48-h and 72-h stage (Figure 4a). Comparing the effects of 10 μg and 50 μg of pCMV-Ad, no significant difference in Adipo levels was seen (142.8 ± 26.1 vs. 143.9 ± 29.1 μg/ml) 24 h post-injection. Since Adipo levels seemed to plateau (Figure 4a), 10 μg of pCMV-Ad was used in subsequent experiments except for the experiment shown in Figure 5a. All mice had been fasted for 3 h prior to pCMV-Ad injection or blood sampling.

Western blot analysis and ELISA were used to quantify the induced Adipo that had been expressed in the serum, liver and muscle of STZ-induced diabetic mice. After transfection of 10 μg of pGL3-basic, Adipo was not detected in liver tissue, and the Adipo level in muscle was 5.24 ± 1.34 μg/g (Figure 4b). After transfection of 10 μg of pCMV-Ad, Adipo levels were 112.7 ± 41.3 μg/g in liver and 16.04 ± 2.56 μg/g in muscle (Figure 4b). Twenty-four hours after injection of 10 μg of pCMV-Ad, non-diabetic mice exhibited Adipo levels of 156.0 ± 1.68 μg/ml in blood serum, 273.1 ± 13.5 μg/g in liver tissues, and 6.64 ± 0.86 μg/g in muscle tissues (data not shown). The level of Adipo in liver was significantly higher than that in muscle, in STZ-induced diabetic mice as well as non-diabetic mice, after injection of 10 μg of pCMV-Ad, which suggested that pCMV-Ad was mainly expressed in the liver and the induced Adipo protein was then secreted from that organ into the bloodstream.

Hepatic Adipo expression reduces serum glucose and triglyceride levels

The effect of hepatic Adipo expression on glycemia was observed by measuring serum glucose levels in STZ-induced diabetic mice after hydrodynamic injections of 10 μg of pCMV-luc, 10 μg of pGL3-basic, or 1, 5, 10 and 50 μg of pCMV-Ad (Figure 5a). Mice transfected with either pGL3-basic or pCMV-Ad showed high glucose levels of over 600 mg/dl prior to injection. By 24 h, glucose concentration in mice transfected with 1 or 5 μg of pCMV-Ad 24 h had decreased to 77 and 75% of the pre-injection levels, and those injected with 10 or 50 μg of pCMV-Ad had decreased to 58 and 49% (531 ± 21 and 410 ± 73 mg/dl, respectively, $P < 0.05$) of the pre-injection concentration, while those injected with pGL3-basic or pCMV-luc did not exhibit such a marked reduction (802 ± 47 mg/dl). Although the glucose-lowering effect caused by 10 μg of pCMV-Ad did not extend beyond 48 h, the effect of 50 μg of pCMV-Ad was sustained beyond 48 h and up to 72 h, after which serum glucose concentration returned to pre-injection levels. Furthermore, the glucose-lowering effect of a dose of 10 μg of pCMV-Ad was evident in non-diabetic mice because, at 24 h post-injection,

DOI: 10.1002/jgm

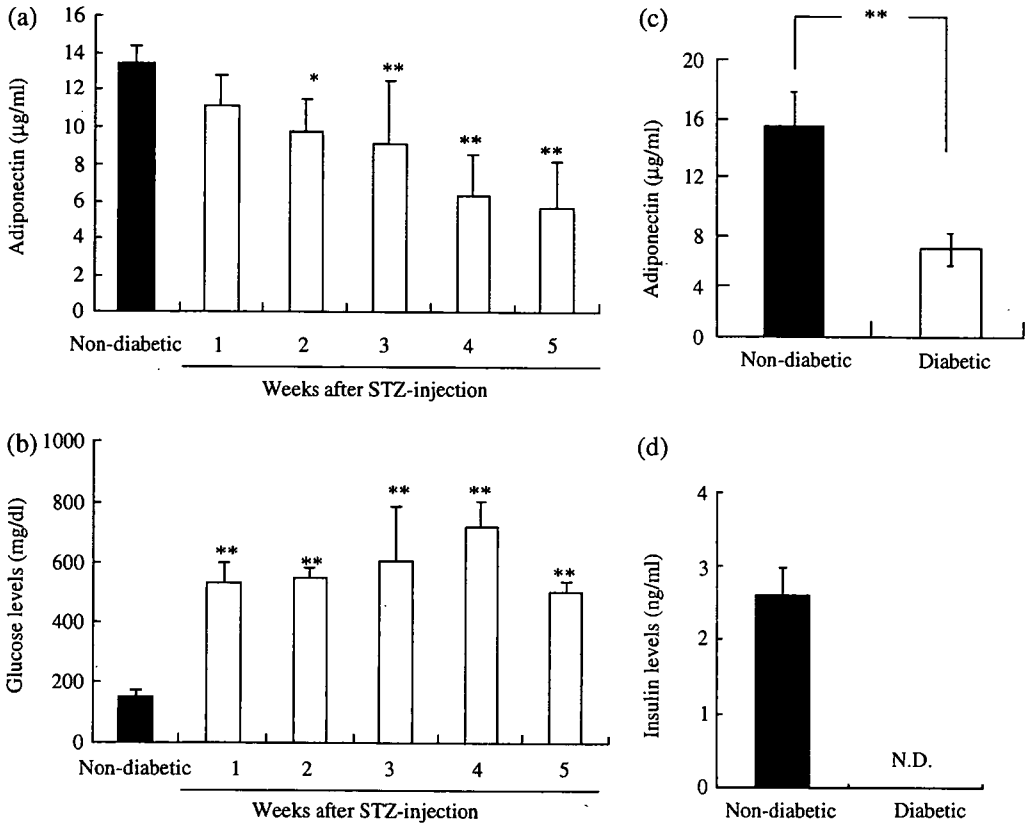

Figure 3. Serum Adipo, glucose and insulin levels in non-diabetic and type 1 diabetic model mice. Time-dependent change of serum Adipo, glucose levels in non-diabetic and type 1 diabetic model mice after treatment with STZ. Serum Adipo levels (a) and glucose levels (b) in non-diabetic and STZ-induced diabetic mice; $n = 7$ for non-diabetic mice (■); $n = 5$ for diabetic mice (□) ($^*P < 0.05$; $^{**}P < 0.01$, compared with non-diabetic mice). Serum Adipo level in STZ-induced diabetic mice was measured once a week for 5 weeks after STZ treatment. Each bar represents the mean ± S.D. (c) Serum Adipo levels in non-diabetic (■) and STZ-induced diabetic mice (□); $n = 4$ for non-diabetic mice; $n = 7$ for diabetic mice 4 to 6 weeks after treatment of STZ ($^{**}P < 0.01$). Each bar represents the mean ± S.E. (d) Serum insulin levels in non-diabetic (■) and STZ-induced diabetic mice (□) 4 to 6 weeks after treatment of STZ; $n = 3$ for each group. Each bar represents the mean ± S.D. For (a–d), each animal was fasted for 3 h before a blood sample was taken. N.D.: not detected. In subsequent experiments, mice held for 4 to 6 weeks after treatment with STZ were used as STZ-induced diabetic mice

serum glucose had dropped from 170.4 ± 9.96 mg/dl to 110.8 ± 11.7 mg/dl (data not shown).

The effect of increasing serum Adipo on serum glucose levels was at its peak 24 h post-injection (Figure 5a) and serum concentrations of insulin, glucagon and triglyceride (TG), as well as AdipoR1 and AdipoR2 mRNA in the liver, were measured at this stage of the experiment. No insulin was detected in STZ-induced diabetic mice 24 h after transfection with either pGL3-basic or pCMV-Ad (data not shown). Serum glucagon levels of STZ-induced diabetic mice injected with 10 μg of pCMV-Ad showed a 40% increase in serum glucagon levels before injection, and this effect could be associated with a recovery in glucose levels (Figure 5b). Moreover, serum TG levels decreased 60% ($P < 0.05$, compared with before injection; Figure 5c), and AdipoR1 and AdipoR2 mRNA levels in the liver did not change (data not shown). These results demonstrated that high levels of Adipo in the liver had reduced the serum concentrations of glucose and TG, and that these effects had occurred even when insulin was not detected.

Adipo enhances glucose uptake in the liver

The glucose-lowering effect of Adipo was investigated by measuring glucose uptake in heart, liver and muscle tissues using a planar positron imaging system to visualize 18-fluorodeoxyglucose (FDG) after *in vivo* injections of either pGL3-basic or pCMV-Ad. FDG injected into the tail vein quickly reached the heart, then distributed from the liver toward the kidneys and, finally, toward the bowels. Mice with STZ-induced diabetes that had been injected with pCMV-Ad showed higher glucose accumulation in the liver, but not in muscle, for the last 20 min of the 60 min scan, when compared to similar mice injected with control plasmid (Figure 6a). In contrast, glucose accumulation in the liver was not seen after injecting non-diabetic mice with pCMV-Ad or control plasmid (data not shown). Liver FDG levels in STZ-induced diabetic mice transfected with pCMV-Ad were higher than those injected with pGL3-basic. Twenty-four hours post-injection, hepatic tissues of diabetic mice injected

DOI: 10.1002/jgm

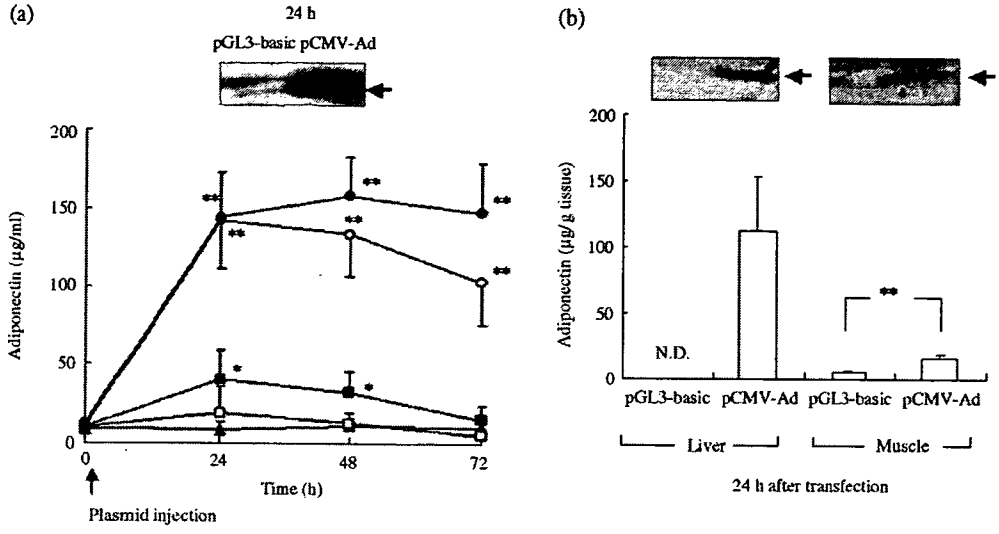

Figure 4. Adipo expression after hydrodynamic injection of pCMV-Ad in STZ-induced diabetic mice. (a) Serum Adipo levels after injection of 10 μg of pGL3-basic (▲) or 1 μg (□), 5 μg (■), 10 μg (○) or 50 μg of pCMV-Ad (●); $n = 3$–6 for each group. Each bar represents the mean ± S.D. (*$P < 0.05$; **$P < 0.01$, compared with before injection). Western blot analyses of Adipo in serum 24 h after injection of 10 μg of pGL3-basic or pCMV-Ad. (b) Adipo levels and Western blot analyses of Adipo in liver and muscle 24 h after injection of 10 μg of pGL3-basic or pCMV-Ad; $n = 3$ for each group. Each bar represents the mean ± S.D. ($P < 0.01$, compared with pGL3-basic). N.D.: not detected**

with pCMV-Ad showed slightly stronger AMPK activation than similar mice injected with pGL3-basic (data not shown). Data suggests that high levels of Adipo expression in the liver were associated with increased hepatic glucose uptake (Figure 6b).

Discussion

Serum Adipo levels in STZ-induced diabetic mice were lower than non-diabetic mice, and could be increased by hydrodynamic injection of pCMV-Ad, which reduced serum glucose and TG levels in the absence of insulin. Furthermore, diabetic mice with higher levels of Adipo expression by injection exhibited higher hepatic glucose uptake than those featuring low levels of Adipo expression.

Adipo levels in STZ-induced diabetic mice were less than those in non-diabetic mice 4–6 weeks after treatment with STZ in mice aged 4 weeks. This effect neither appeared up to 1 week after the treatment with STZ in mice aged 4 weeks, despite persistently high serum glucose levels. Although circulating levels of Adipo may be diminished in insulin-resistant illnesses, such as obesity [21] and type 2 diabetes [22,23], Adipo levels in type 1 diabetes increased [24] and did not [25]. Adipo levels in STZ-induced diabetic mice after treatment with STZ in mice did not change significantly [26,27]. However, recently, it has been reported that Adipo levels in STZ-induced diabetic rats were suppressed when compared with non-diabetic rats [28]. Age and weight of mice treated with STZ, as well as time after treatment, may greatly affect Adipo levels in STZ-induced diabetic mice. Adipo has multiple biological functions and the exact mechanism behind these differences remains unclear. The reduction of serum Adipo levels in STZ-induced diabetic mice may be related to atrophy of adipocytes and/or other diseases that might be induced by diabetes mellitus.

Hydrodynamic injection has proven to be a very efficient method for hepatic delivery of genes into mice [11,12]. In this study, serum and hepatic Adipo levels in STZ-induced diabetic mice were elevated after hydrodynamic injection of pCMV-Ad had caused high levels of Adipo expression (Figures 4a and 4b). High levels of Adipo expression were sustained for 3 days post-injection and peak expression (142.8 ± 26.1 μg/ml at 10 μg dose/mouse) was seen at the 24-h mark. Corresponding with changes in Adipo expression seen at this mark, serum glucose levels in STZ-induced diabetic mice transfected with 10 and 50 μg of pCMV-Ad had been reduced by more than 50%. Adenovirus-mediated Adipo transfection into Wistar rats increased serum Adipo levels to approximately 70 μg/ml 7 days after intravenous injection, but did not decrease glucose levels [10]. Intraperitoneal injection of recombinant Adipo protein caused a 2- to 3-fold increase in circulating Adipo levels to over 125 μg/ml after 4 h, and triggered a transient decrease in glucose levels in non-diabetic mice, STZ-induced diabetic mice, and non-obese diabetic mice (NOD) (more than 50% decrease before injection for all of them) [26,29]. Consequently, the delivery of Adipo genes to the liver has been shown to be effective in decreasing glucose levels, compared to an injection of Adipo protein. This study provides the first *in vivo* evidence that Adipo expression via pCMV-Ad genes can reduce serum glucose levels in the absence of insulin.

Expression of pCMV-Ad brought about a decrease in serum glucose without changing the concentration of

DOI: 10.1002/jgm

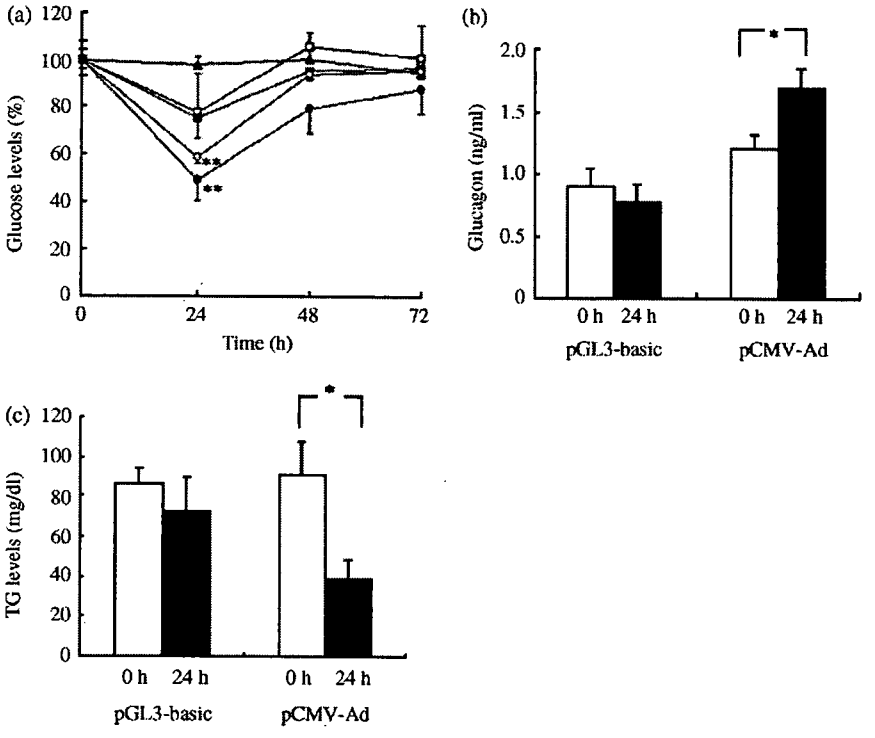

Figure 5. Hydrodynamic injection of pCMV-Ad decreased glucose and TG levels in serum in STZ-induced diabetic mice. (a) Serum glucose levels after injection of 10 μg of pGL3-basic (▲) or 1 μg (□), 5 μg (■), 10 μg (○) or 50 μg of pCMV-Ad (●). Each bar represents the mean ± S.E.; $n = 3–8$. (b) Serum glucagon levels at 0 h (□) or 24 h (■) after injection of 10 μg of pGL3-basic or pCMV-Ad. Each bar represents the mean ± S.E.; $n = 4$. (c) Serum TG levels 0 h (□) or 24 h (■) after injection of 10 μg of pGL3-basic or pCMV-Ad. Each bar represents the mean ± S.E.; n = 4–5. (*$P < 0.05$; **$P < 0.01$, compared with before injection). Each animal shown was fasted for 3 h before the experiment and before a blood sample was taken

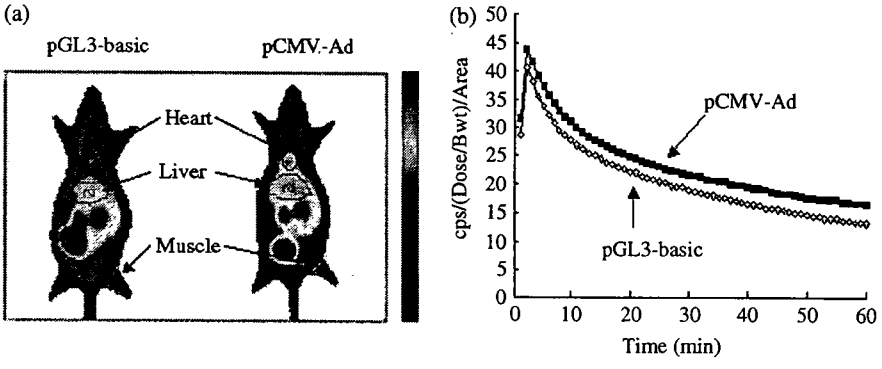

Figure 6. Dynamic change in FDG uptake, measured using a planar positron imaging system (PPIS), 18–24 h after hydrodynamic injection of 10 μg of pGL3-basic or pCMV-Ad into STZ-induced diabetic mice. (a) Distribution of FDG in heart, liver and muscle tissues of STZ-induced diabetic mice. Each image is a composite of accumulated data for the last 20 min of the session. (b) Time-activity curves (TAC) of radioactivity in the liver from 0 to 60 min; $n = 3$ for each group. Variations between experiments are shown at each point. Each animal was fasted for more than 12 h before the experiment. CPS: counts per second of the liver frame in (a) were normalized by dividing body weight (g) and unit area (mm^2)

AdipoR1 or AdipoR2 mRNA in the liver. Inukai *et al.* and Tsuchida *et al.* showed that treatment with STZ led to a reduction in plasma insulin and, at the same time, caused a marked increase in AdipoR1 and AdipoR2 mRNA levels in muscle tissues [27,30], without significantly altering AdipoR2 mRNA levels in the liver [27,31]. The decrease in serum glucose concentration triggered a subsequent rise in glucagon levels. Since serum insulin was not detected in STZ-diabetic mice, it seems that the stimulating effect of glucagon on glucose level may be significant, and at 24 h after transfection of Adipo, the glucagon level was significantly elevated. This increase of glucagon level in the absence of insulin may act continuously, thereby resulting in restoration of the glucose level at 48 h. This finding correlated with a previous investigation by Berg *et al.* [26], which showed that glucagon and other potential counter-regulatory mechanisms were capable of instigating a recovery in basal glucose levels, and

DOI: 10.1002/jgm

that over-expression of Adipo caused a subsequent down-regulation in serum TG levels. In the end, the presence of Adipo resulted in a reduction of liver TG in obese and type 2 diabetic mice [32] by increasing fatty-acid oxidation.

The glucose-lowering effect of recombinant Adipo protein in NOD mice may be due to an increase in sensitivity to insulin [26]. In this study, STZ-induced diabetic mice exhibited undetectable insulin levels (<0.25 ng/ml), as well as high levels of Adipo expression, and experienced a decrease in glucose levels after transfection of pCMV-Ad.

Serum Adipo may play a role in the regulation of glucose homeostasis. Adipo expression decreased glucose levels and suppressed hepatic glucose production [29]. Under these conditions, serum glucose levels were predominantly governed by hepatic glucose output and input. Diabetic mice with high levels of Adipo expression by injection were able to increase their hepatic glucose uptake above those with low Adipo expression. In conjunction with AMPK activation, Adipo stimulated fatty-acid oxidation and glucose uptake in skeletal muscle [33–35], reduced the availability of gluconeogenesis components, such as glucose-6-phosphatase in hepatocytes [36], and reduced serum glucose levels in mice [16,26,31,37]. Increased rates of glucose uptake in diabetic mice have been seen in muscle tissues, but not in the liver. Here, it seems that Adipo expression actually stimulated glucose uptake in the liver.

When investigating the insulin-independent glucose-lowering effect, treatment with AICAR or transfection with pCMV-Ad confirmed the presence of AMPK activation in HepG2 cells. Cells treated with AICAR did not increase glucose uptake, but cells transfected with pCMV-Ad significantly increased glucose uptake when compared with those transfected with pGL3-basic (Figure 2c). These findings suggest that Adipo-associated increases in hepatic glucose uptake may not be mediated by AMPK activation in diabetic mice expressing Adipo. In addition, the Adipo gene delivery to the liver in diabetic mice was able to alter hepatic glucose uptake, and the glucose-lowering effect exerted by Adipo on hepatocytes took place even in the absence of insulin. Although this glucose-lowering effect did not seem to be dependent on insulin, we cannot rule out the possibility that very low insulin levels in STZ-induced diabetic mice (<0.25 ng/ml) might be present and could still affect the ability of Adipo to influence serum glucose levels [26].

Thus, we have shown for the first time that hyperglycemia in type 1 diabetes can be alleviated by delivery of Adipo plasmid DNA to liver. Recently, alternative techniques to hydrodynamic injection for clinical applications were reported [38,39]. This type of gene delivery to the liver provides a different approach to gene therapy of type 1 and type 2 diabetes.

Acknowledgements

This project was partly supported by a grant, the Open Research Center Project, from the Promotion and Mutual Aid Corporation for Private Schools of Japan, and a Grant-in-aid for Scientific Research from the Ministry of Education, Culture, Sports, Science, and Technology of Japan.

References

1. Maeda K, Okubo K, Shimomura I, Funahashi T, Matsuzawa Y, Matsubara K. cDNA cloning and expression of a novel adipose specific collagen-like factor, apM1 (AdiPose Most abundant Gene transcript 1). *Biochem Biophys Res Commun* 1996; **221**: 286–289.
2. Nakano Y, Tobe T, Choi-Miura NH, Mazda T, Tomita M. Isolation and characterization of GBP28, a novel gelatin-binding protein purified from human plasma. *J Biochem (Tokyo)* 1996; **120**: 803–812.
3. Hu E, Liang P, Spiegelman BM. AdipoQ is a novel adipose-specific gene dysregulated in obesity. *J Biol Chem* 1996; **271**: 10697–10703.
4. Scherer PE, Williams S, Fogliano M, Baldini G, Lodish HF. A novel serum protein similar to C1q, produced exclusively in adipocytes. *J Biol Chem* 1995; **270**: 26746–26749.
5. Kahn BB, Flier JS. Obesity and insulin resistance. *J Clin Invest* 2000; **106**: 473–481.
6. Shulman GI. Cellular mechanisms of insulin resistance. *J Clin Invest* 2000; **106**: 171–176.
7. Yamauchi T, Kamon J, Ito Y, *et al.* Cloning of adiponectin receptors that mediate antidiabetic metabolic effects. *Nature* 2003; **423**: 762–769.
8. Yamauchi T, Kamon J, Waki H, *et al.* The fat-derived hormone adiponectin reverses insulin resistance associated with both lipoatrophy and obesity. *Nat Med* 2001; **7**: 941–946.
9. Shklyaev S, Aslanidi G, Tennant M, *et al.* Sustained peripheral expression of transgene adiponectin offsets the development of diet-induced obesity in rats. *Proc Natl Acad Sci U S A* 2003; **100**: 14217–14222.
10. Satoh H, Nguyen MT, Trujillo M, *et al.* Adenovirus-mediated adiponectin expression augments skeletal muscle insulin sensitivity in male Wistar rats. *Diabetes* 2005; **54**: 1304–1313.
11. Liu F, Song Y, Liu D. Hydrodynamics-based transfection in animals by systemic administration of plasmid DNA. *Gene Ther* 1999; **6**: 1258–1266.
12. Zhang G, Budker V, Wolff JA. High levels of foreign gene expression in hepatocytes after tail vein injections of naked plasmid DNA. *Hum Gene Ther* 1999; **10**: 1735–1737.
13. Jiang J, Yamato E, Miyazaki J. Long-term control of food intake and body weight by hydrodynamics-based delivery of plasmid DNA encoding leptin or CNTF. *J Gene Med* 2003; **5**: 977–983.
14. He CX, Shi D, Wu WJ, *et al.* Insulin expression in livers of diabetic mice mediated by hydrodynamics-based administration. *World J Gastroenterol* 2004; **10**: 567–572.
15. Park JH, Lee M, Kim SW. Non-viral adiponectin gene therapy into obese type 2 diabetic mice ameliorates insulin resistance. *J Control Release* 2006; **114**: 118–125.
16. Yamauchi T, Kamon J, Minokoshi Y, *et al.* Adiponectin stimulates glucose utilization and fatty-acid oxidation by activating AMP-activated protein kinase. *Nat Med* 2002; **8**: 1288–1295.
17. Hattori Y, Maitani Y. Folate-linked nanoparticle-mediated suicide gene therapy in human prostate cancer and nasopharyngeal cancer with herpes simplex virus thymidine kinase. *Cancer Gene Ther* 2005; **12**: 796–809.
18. Kamata K, Sugiura M, Kojima S, Kasuya Y. Preservation of endothelium-dependent relaxation in cholesterol-fed and streptozotocin-induced diabetic mice by the chronic administration of cholestyramine. *Br J Pharmacol* 1996; **118**: 385–391.
19. Takamatsu H, Kakiuchi T, Noda A, *et al.* An application of a new planar positron imaging system (PPIS) in a small animal: MPTP-induced parkinsonism in mouse. *Ann Nucl Med* 2004; **18**: 427–431.
20. Uchida H, Okamoto T, Ohmura T, *et al.* A compact planar positron imaging system. *Nucl Instrum Methods in Phys Res, Sect A* 2004; **516**: 564–574.
21. Arita Y, Kihara S, Ouchi N, *et al.* Paradoxical decrease of an adipose-specific protein, adiponectin, in obesity. *Biochem Biophys Res Commun* 1999; **257**: 79–83.

22. Weyer C, Funahashi T, Tanaka S, *et al.* Hypoadiponectinemia in obesity and type 2 diabetes: close association with insulin resistance and hyperinsulinemia. *J Clin Endocrinol Metab* 2001; **86**: 1930–1935.
23. Stefan N, Stumvoll M, Vozarova B, *et al.* Plasma adiponectin and endogenous glucose production in humans. *Diabetes Care* 2003; **26**: 3315–3319.
24. Imagawa A, Funahashi T, Nakamura T, *et al.* Elevated serum concentration of adipose-derived factor, adiponectin, in patients with type 1 diabetes. *Diabetes Care* 2002; **25**: 1665–1666.
25. Morales A, Wasserfall C, Brusko T, *et al.* Adiponectin and leptin concentrations may aid in discriminating disease forms in children and adolescents with type 1 and type 2 diabetes. *Diabetes Care* 2004; **27**: 2010–2014.
26. Berg AH, Combs TP, Du X, Brownlee M, Scherer PE. The adipocyte-secreted protein Acrp30 enhances hepatic insulin action. *Nat Med* 2001; 7: 947–953.
27. Inukai K, Nakashima Y, Watanabe M, *et al.* Regulation of adiponectin receptor gene expression in diabetic mice. *Am J Physiol Endocrinol Metab* 2005; **288**: E876–E882.
28. Thule PM, Campbell AG, Kleinhenz DJ, *et al.* Hepatic insulin gene therapy prevents deterioration of vascular function and improves adipocytokine profile in STZ-diabetic rats. *Am J Physiol Endocrinol Metab* 2006; **290**: E114–E122.
29. Combs TP, Berg AH, Obici S, Scherer PE, Rossetti L. Endogenous glucose production is inhibited by the adipose-derived protein Acrp30. *J Clin Invest* 2001; **108**: 1875–1881.
30. Tsuchida A, Yamauchi T, Ito Y, *et al.* Insulin/Foxo1 pathway regulates expression levels of adiponectin receptors and adiponectin sensitivity. *J Biol Chem* 2004; **279**: 30817–30822.
31. Tsuchida A, Yamauchi T, Kadowaki T. Nuclear receptors as targets for drug development: molecular mechanisms for regulation of obesity and insulin resistance by peroxisome proliferator-activated receptor gamma, CREB-binding protein, and adiponectin. *J Pharmacol Sci* 2005; **97**: 164–170.
32. Fruebis J, Tsao TS, Javorschi S, *et al.* Proteolytic cleavage product of 30-kDa adipocyte complement-related protein increases fatty acid oxidation in muscle and causes weight loss in mice. *Proc Natl Acad Sci U S A* 2001; **98**: 2005–2010.
33. Hardie DG, Carling D, Carlson M. The AMP-activated/SNF1 protein kinase subfamily: metabolic sensors of the eukaryotic cell? *Annu Rev Biochem* 1998; **67**: 821–855.
34. Winder WW, Hardie DG. AMP-activated protein kinase, a metabolic master switch: possible roles in type 2 diabetes. *Am J Physiol* 1999; **277**: E1–E10.
35. Mu J, Brozinick JT Jr, Valladares O, Bucan M, Birnbaum MJ. A role for AMP-activated protein kinase in contraction- and hypoxia-regulated glucose transport in skeletal muscle. *Mol Cell* 2001; 7: 1085–1094.
36. Lochhead PA, Salt IP, Walker KS, Hardie DG, Sutherland C. 5-Aminoimidazole-4-carboxamide riboside mimics the effects of insulin on the expression of the 2 key gluconeogenic genes PEPCK and glucose-6-phosphatase. *Diabetes* 2000; **49**: 896–903.
37. Kadowaki T, Yamauchi T. Adiponectin and adiponectin receptors. *Endocr Rev* 2005; **26**: 439–451.
38. Alino SF, Herrero MJ, Noguera I, Dasi F, Sanchez M. Pig liver gene therapy by noninvasive interventionist catheterism. *Gene Ther* 2007; **14**: 334–343.
39. Tada M, Hatano E, Taura K, *et al.* High volume hydrodynamic injection of plasmid DNA via the hepatic artery results in a high level of gene expression in rat hepatocellular carcinoma induced by diethylnitrosamine. *J Gene Med* 2006; **8**: 1018–1026.

Low-Molecular-Weight Polyethylenimine Enhanced Gene Transfer by Cationic Cholesterol-Based Nanoparticle Vector

Yoshiyuki HATTORI* and Yoshie MAITANI

Institute of Medicinal Chemistry, Hoshi University; 2–4–41 Ebara, Shinagawa-ku, Tokyo 142–8501, Japan.
Received May 8, 2007; accepted June 25, 2007; published online June 26, 2007

Both polyethylenimine (PEI) polymers and cationic nanoparticles have been widely used for non-viral DNA transfection. Previously, we reported that cationic nanoparticles composed of cholesteryl-3β-carboxyamidoethylene-*N*-hydroxyethylamine and Tween 80 (NP-OH) could deliver plasmid DNA (pDNA) with high transfection efficiency. To increase the transfection activity of NP-OH, we investigated the potential synergism of PEI and NP-OH for the transfection of DNA into human prostate tumor PC-3, human cervices tumor Hela, and human lung adenocarcinoma A549 cells. The transfection efficiency with low-molecular PEI (MW 600) was low, but that with a combination of NP-OH and PEI was higher than with NP-OH alone, being comparable to commercially available lipofectamine 2000 and lipofectamine LTX, with very low cytotoxicity. Low-molecular weight PEI could not compact pDNA in size, but rather might help to dissociate pDNA from the complex and release pDNA from the endosome to cytoplasm by the proton sponge effect. Therefore, the combination of cationic cholesterol-based nanoparticles and a low-molecular PEI has potential as a non-viral DNA vector for gene delivery.

Key words cationic nanoparticle; gene delivery; transfection; cholesteryl-3β-carboxyamidoethylene-*N*-hydroxyethylamine; polyethylenimine; nanoplex; PC-3 cell

Gene delivery has become an increasingly important strategy for treating a variety of human diseases, including cancer.[1] It is important to develop gene delivery vectors with strong transfection activity and low toxicity for applications *in vivo*. Many different cationic lipids have been synthesized for delivering genes into cells. The use of cationic cholesterol derivatives is justified by their high transfection activity and low toxicity.[2,3] Cholesteryl-3β-carboxyamidoethylene-*N*-hydroxyethylamine (OH-Chol), having a hydroxyethyl group at the amino terminal, is a cationic cholesterol derivative with good transfection efficiency for plasmid DNA (pDNA) delivery.[2]

Polyethylenimines (PEIs) are a large group of non-viral vectors that have been shown to be capable of delivering pDNA into various cell lines.[4] PEI/pDNA complexes (polyplex) are taken up by a variety of cells *via* endocytosis, enter the endosomal compartment, and are finally released due to their buffer capacity *via* the so-called "proton sponge mechanism".[5] PEI has the ability to capture protons that are pumped into endosomes. This is followed by a passive influx of chloride ions into endosomes and subsequent osmotic swelling and disruption of the endosomes. This permits the escape of endocytosed DNA.[5,6] The transfection efficiency of PEI increases with increasing molecular weight. The low-molecular weight PEIs (600, 1200, 1800) are virtually ineffective.[7] The smallest PEI that has been used in gene transfection has been 11900.[8] Large PEIs, such as PEI 25K (average MW 25000)[9—12] and PEI 80K (average MW 80000),[5,9,11] have been used successfully in transfection studies. PEIs with a mean molecular weight of less than 2000 are inactive as transfection agents, but can be used in combination with cationic liposomes.[13,14]

Cationic liposomes are widely used as gene transfection reagents, and bind electrostatically to negatively charged DNA to form complexes. These lipoplexes enter the cells *via* endocytosis. After endocytosis, the pDNA must escape from the endosomes into the cytoplasm. PEI is able to enhance gene transfer by helping to disrupt the endosomal membrane.[4] The use of low-molecular weight PEIs (MW 700, 2000) with liposomes such as dioleoyloxypropyl trimethylammonium methylsulfate (DOTAP) liposome, lipofectamine and polycationic liposome Dosper resulted in a synergistic increase in the transfection efficiency in rat smooth muscle or rat glioma C6 cells, but that with cationic dendrimers (Superfect) did not.[13,15] Among them, the combination of Dosper liposome and low-molecular PEI caused the most effective transfection synergism. However, it was not clear whether cationic nanoparticles could enhance transfection efficiency in combination with PEI.

We previously reported that cationic nanoparticles composed of OH-Chol and Tween 80 (NP-OH) could deliver pDNA with high transfection efficiency when the nanoparticle/pDNA complex (nanoplex) was formed in a 50 mM NaCl solution.[16,17] In this study, to increase the transfection efficiency of NP-OH, we evaluated the potential synergism of PEI of low- (average MW 600, 1800) or high- (average MW 10000; 10K) molecular weight and NP-OH for pDNA transfection. The transfection resulted in efficient DNA transfer in human prostate tumor PC-3, human cervices tumor Hela, and human lung adenocarcinoma A549 cells as a ternary complex with low-molecular weight PEI 600, NP-OH, and pDNA.

MATERIALS AND METHODS

Preparation of pDNA The plasmid pCMV-Gluc control encoding secretable *Gaussia* luciferase (Gluc) under the control of the CMV promoter was purchased from New England Biolabs (MA, U.S.A.). A protein-free preparation of the plasmid was purified following alkaline lysis using maxiprep columns (Qiagen, Hilden, Germany).

Preparation of Nanoparticles, Nanoplexes, and Ternary Complexes The synthesis of OH-Chol was done as previously described.[16] NP-OH formulation consisted of 1 mg/ml of OH-Chol as a cationic lipid and 5 mol% of Tween 80 (NOF Co., Ltd., Tokyo, Japan). NP-OH nanoparticles were

* To whom correspondence should be addressed. e-mail: yhattori@hoshi.ac.jp

prepared with lipids (*e.g.* OH-Chol : Tween 80=10 : 1.3, weight (mg)) in 10 ml of water by the modified ethanol injection method as previously described.[16]

The charge ratio (+/−) of NP-OH/pDNA is expressed as the nitrogen of cationic lipid/DNA phosphate ratio. The NP-OH/pDNA complex (nanoplex) was formed by the addition of NP-OH to 2 μg of pDNA in water or 50 μl of 50 mM NaCl solution with gentle shaking and leaving at room temperature for 10 min.

For preparation of the NP-OH/PEI/pDNA complex (ternary complex), we used 3 kinds of branched PEIs (MW 600, 1800, 10000 (10K), Wako Chemicals, Osaka, Japan). The charge ratio (+/−) of PEI/pDNA is expressed as the PEI amine nitrogen/DNA phosphate ratio. PEIs were used with charge ratios (+/−) of 1, 2 and 3, and NP-OH nanoparticles had cationic lipid/DNA ratios of between 1 and 3. Briefly, to form PEI/pDNA complexes (polyplexes), pDNA was combined with the PEI solution to achieve charge ratios (+/−) of 1, 2, and 3 in water or 5—50 mM NaCl solution and incubated for 10 min. Ternary complexes were formed by the addition of nanoparticles to the polyplex solution at the NP-OH/DNA ratios mentioned above, and left at room temperature for another 10 min. The particle size distributions and ζ-potentials were measured with an ELS-Z2 (Otsuka Electronics Co., Ltd., Osaka, Japan), at 25 °C after diluting the dispersion to an appropriate volume with water. The average size and ζ-potential of NP-OH were approximately 120—130 nm and +45—50 mV, respectively.

Cell Culture PC-3 cells were supplied by the Cell Resource Center for Biomedical Research, Tohoku University (Miyagi, Japan). Hela cells were obtained from the European Collection of Cell Culture (Wiltshire, U.K.). A549 cells were a gift from Oncotherapy Science (Tokyo, Japan). The cells were grown in RPMI-1640 medium (Invitrogen Corp., Carlsbad, CA, U.S.A.) supplemented with 10% heat-inactivated fetal bovine serum (FBS) (Invitrogen Corp., Carlsbad, CA, U.S.A.) and kanamycin (100 μg/ml) at 37 °C in a 5% CO_2 humidified atmosphere.

Secreted Gaussia Luciferase Assay PC-3, Hela, and A549 cells were plated into 96-well culture dishes. For transfection, nanoplexes, polyplexes and ternary complexes were diluted in 1 ml of medium supplemented with 10% FBS and then 100 μl of the mixture were incubated with the cells for 24 and 48 h. Lipofectamine 2000 and lipofectemine LTX lipoplexes (Invitrogen Corp.) were prepared according to the manufacturer's protocol. Activity of secreted *Gaussia* luciferase in medium was measured as counts per second (cps)/culture medium (μl) using a Gaussia Luciferase Assay Kit (New England BioLabs, Inc., MA, U.S.A.) according to the manufacturer's directions.

Gel Retardation Assay One microgram of pDNA was mixed with aliquots of PEI 600, 1800, 10K, and NP-OH (1 to 3 charge equivalents of cationic polymer or lipid) in 50 mM NaCl solution. After a 10-min incubation, the polyplexes and nanoplexes were analyzed by 1.5% agarose gel electrophoresis in Tris-Borate-EDTA (TBE) buffer and visualized by ethidium bromide staining as previously described.[16]

Cytotoxicity PC-3, Hela, and A549 cells were plated into 96-well culture dishes. Cytotoxicity upon transfection using nanoplexes, ternary complexes, lipofectamine 2000, or lipofectamine LTX was evaluated with a cell proliferation assay kit (Dojindo, Kumamoto, Japan). Nanoplexes and ternary complexes were prepared in 50 mM NaCl solution as described above, and transfected into the cells in medium containing 10% FBS. After 48 h of incubation, the medium was removed, and the cells were treated with a WST-8 (2-(2-methoxy-4-nitrophenyl)-3-(4-nitrophenyl)-5-(2,4-disulfophenyl)-2*H*-tetrazolium, monosodium salt) solution (10 μl) in medium containing serum (100 μl) for 30 min. Cell viability was expressed relative to the absorbance at 450 nm of untransfected cells.

Statistical Analysis Multiple measurement comparisons were performed with an analysis of variance followed by a one-way analysis of variance on ranks with a *post-hoc* Tukey–Kramer test. A p value of 0.05 or less was considered significant.

RESULTS

PEI Polyplex-Mediated Gene Transfer First, the transfection efficiency of the PEI polyplexes formed with PEI 600, 1800, and 10K was evaluated in PC-3 cells. Among the PEI polyplexes formed in water, the PEI 10K polyplex showed higher transfection activity than the PEI 600 and 1800 polyplexes, and its luciferase activity increased in parallel with the increasing charge ratio (+/−) (Fig. 1A). However, the transfection efficiency was significantly lower than that of commercial products. This finding corresponded to the finding that PEIs of low-molecular weights produced low transfection efficiency.[7] The presence of NaCl in the polyplex did not increase transfection efficiency (Fig. 1B).

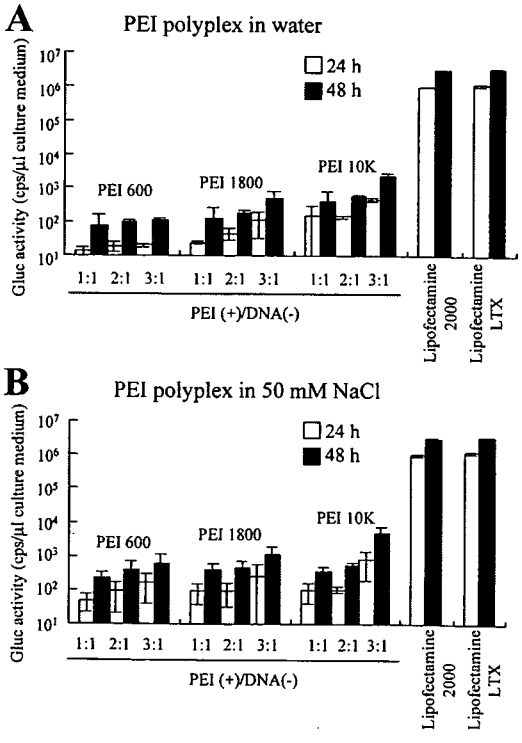

Fig. 1. Effect of Charge Ratio (+/−) of PEI/pDNA Polyplex on Transfection in PC-3 Cells

Polyplexes were formed in water (A) or a 50 mM NaCl solution (B) at charge ratios (+/−) of PEIs to pDNA of 1/1, 2/1 and 3/1. Each column represents the mean±S.D. (n=3).

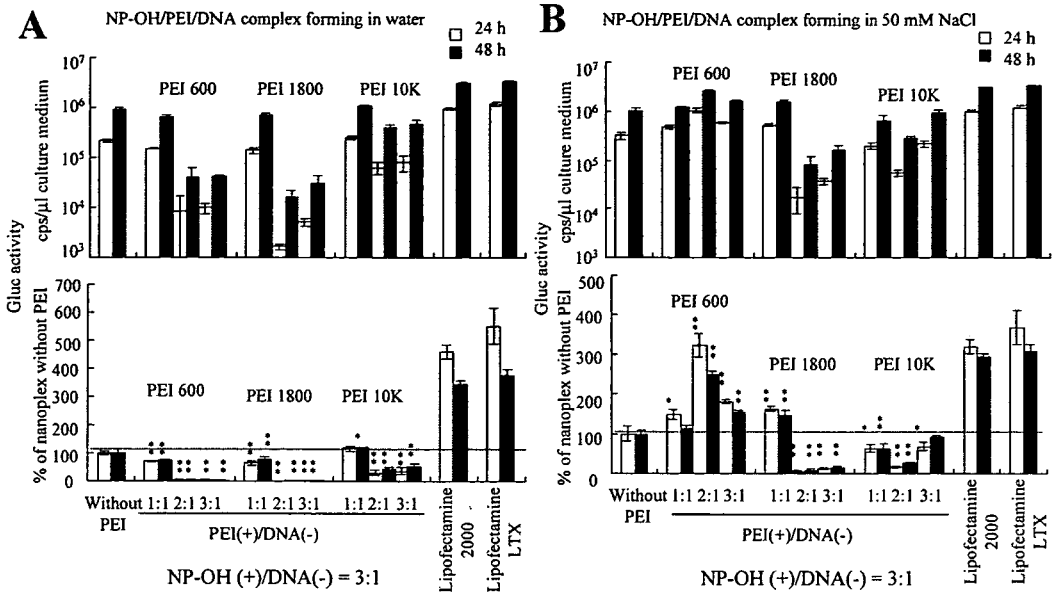

Fig. 2. Effect of Charge Ratio (+/−) of PEI/pDNA in Ternary Complex on Transfection in PC-3 Cells

Using polyplexes formed in water (A) or a 50 mM NaCl solution (B) at charge ratios (+/−) of 1/1, 2/1, and 3/1, the ternary complex was formed at a charge ratio (+/−) of 3/1. $^{**}p<0.01$ and $^{*}p<0.05$, compared with a ternary complex without PEI. Each column represents the mean±S.D. ($n=3$).

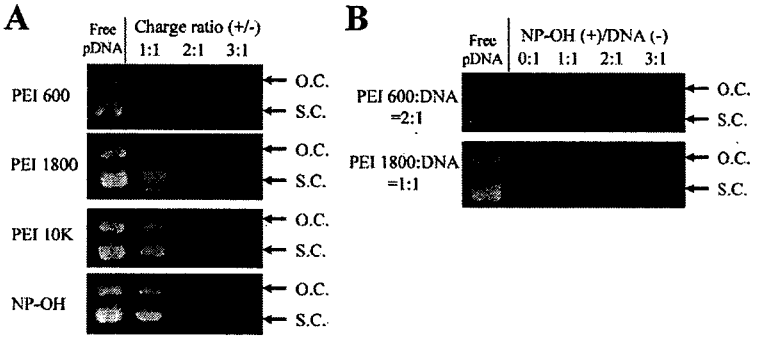

Fig. 3. Association of pDNA with PEI and NP-OH in 50 mM NaCl at Various Charge Ratios (+/−) Was Analyzed Using 1.5% Agarose Gel Electrophoresis

One microgram of pDNA was mixed with aliquots of PEI 600, 1800, 10K or NP-OH at various charge ratios (A). Ternary complexes at charge ratios (+/−) of 2/1 for PEI 600 and 1/1 for PEI 1800 were formed at various charge ratios (+/−) of NP-OH (B). O.C. indicates open circular plasmid; S.C. indicates supercoiled plasmid.

Effect of PEI/pDNA Ratio in Ternary Complex on Transfection The effect on transfection efficiency of different charge ratios (+/−) of the PEI/pDNA in NP-OH ternary complexes was studied (Fig. 2). Charge ratio (+/−) of NP-OH /pDNA ratio of 3/1 was chosen, since this had been effective when used alone.[16,17] Ternary complexes prepared in water were all ineffective in the cells (Fig. 2A). Gluc activity in the culture medium decreased with the increasing charge ratio (+/−) of PEI/pDNA. However, when the ternary complex was prepared in 50 mM NaCl, PEI 600 at a charge ratio (+/−) of 2/1 and PEI 1800 at a charge ratio (+/−) of 1/1 increased transfection efficiency compared with the complex without PEI, *i.e.*, the nanoplex (Fig. 2B). This indicated that a combination of NP-OH and PEI 600 or 1800 could increase transfection when the ternary complex was formed in the presence of a NaCl solution. Therefore, in subsequent experiments, we decided to use PEI 600 at a charge ratio (+/−) of 2/1 and PEI 1800 at a charge ratio (+/−) of 1/1 as optimal PEI/pDNA ratios.

Gel Retardation Assay The association of pDNA with PEI and/or NP-OH was monitored by gel retardation electrophoresis. The migration pattern of pDNA in the polyplex and nanoplex changed when the pDNA was mixed with PEI or NP-OH at charge ratios (+/−) from 1 to 3 in 50 mM NaCl solution. Beyond a charge ratio (+/−) of 2/1 in PEI 600 and 1800 polyplexes, no migration was observed (Fig. 3A). Beyond a charge ratio (+/−) of 3/1 in the PEI 10K polyplex and NP-OH nanoplex, no migration was observed (Fig. 3A). These results indicated that a complete complex was formed above a charge ratio (+/−) of 2/1 in PEI 600 and 1800, and of 3/1 in PEI 10K and NP-OH. Furthermore, in ternary complexes at charge ratios (+/−) of 2/1 for PEI 600 and 1/1 for PEI 1800, no migration was observed beyond a charge ratio (+/−) of NP-OH/pDNA of 1/1 (Fig. 3B), indicating that the ternary complexes of PEI 600 and 1800 used in Fig. 2B were completely formed complexes with pDNA. ζ-Potentials were about +3 and −34 mV when the polyplexes were formed in 50 mM NaCl at a charge ratio (+/−) of 2/1 for PEI 600 and 1/1 for PEI 1800, respectively, and increased to +25 and +35 mV after the formation of ternary complexes at a charge

ratio (+/−) of NP-OH/pDNA of 3/1 (data not shown). This finding also suggested that the pDNA partially neutralized by PEI could be associated with NP-OH.

The Role of NP-OH/pDNA Ratios in Delivery Next, to increase transfection efficiency, we studied the effect of NP-OH/pDNA ratios in combination with PEI 600 or 1800. We used a charge ratio (+/−) of PEI/pDNA of 2/1 for PEI 600 and of 1/1 for PEI 1800 in ternary complexes from the result in Fig. 2B. At a charge ratio (+/−) of NP-OH/pDNA of 3/1, the transfection efficiencies were highest in both PEI 600 and 1800 (Fig. 4). Thereafter, for the optimal PEI 600 and 1800 ternary complexes, we used 3/1 as the charge ratio (+/−) of NP-OH/pDNA. Comparison of the molecular weight of PEI in combination with NP-OH revealed that PEI 600 was more effective than PEI 1800. This finding corresponded with the notion that a low-molecular weight PEI could be used successfully for gene delivery when combined with cationic liposomes.[14]

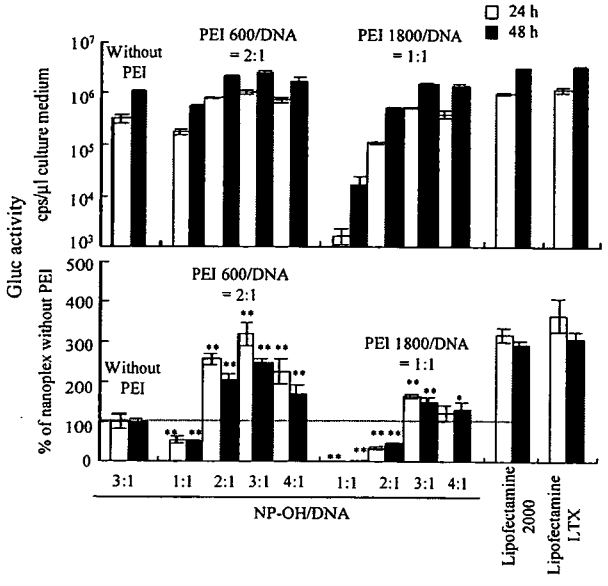

Fig. 4. Effect of Charge Ratio (+/−) of NP/pDNA in Ternary Complex on Transfection in PC-3 Cells

Using polyplexes formed in a 50 mM NaCl solution at charge ratios (+/−) of 2/1 for PEI 600 and 1/1 for PEI 1800, the ternary complex was formed at various charge ratios (+/−) from 1/1 to 4/1. Each column represents the mean±S.D. (n=4). $^{**}p<0.01$ and $^{*}p<0.05$, compared with a ternary complex without PEI.

Effect of Sodium Chloride on the Size of the Ternary Complex We compared the physicochemical properties of ternary complexes at a charge ratio (+/−) of NP-OH/pDNA of 3/1 formed in the presence of various concentrations of NaCl solution. The NP-OH nanoplex formed in water and the 50 mM NaCl solution was about 290 and 820 nm in size, respectively. The PEI 600 polyplex formed in the 50 mM NaCl solution at a charge ratio (+/−) of 2/1 was about 830 nm. The ternary complex formed in water or the 50 mM NaCl solution was about 1500 nm in size (Fig. 5A). A significant difference was not observed in the sizes of the ternary complexes formed between 0 and 100 mM NaCl.

Effect of Sodium Chloride on the Transfection Efficiency of the Ternary Complex We investigated the effect of sodium chloride on the transfection efficiency of ternary complexes in PC-3 cells. The presence of NaCl in the ternary complex increased transfection efficiency in parallel with the increasing concentration of NaCl, and a saturated transfection efficiency was observed at 50 mM NaCl (Fig. 5B). The observed transfection efficiency 24 and 48 h after transfec-

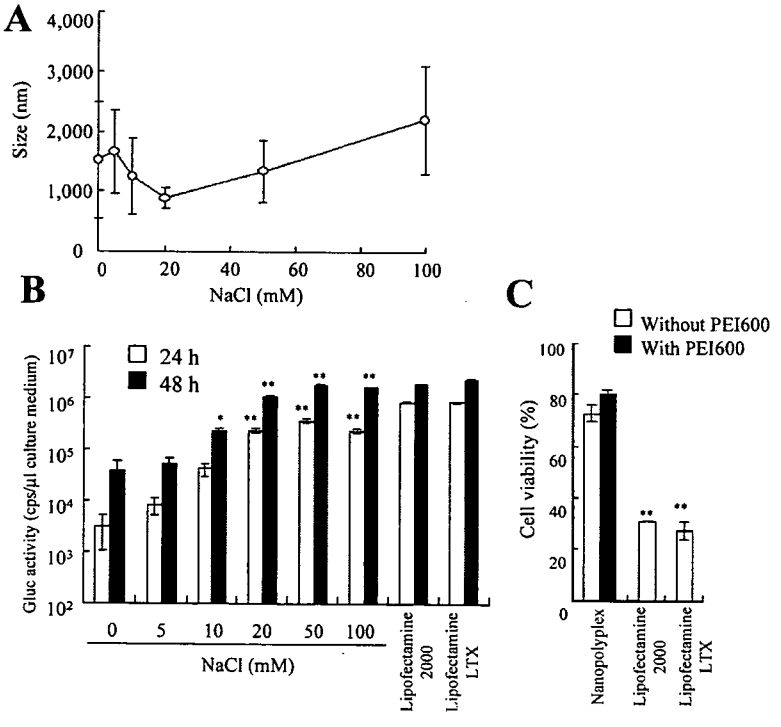

Fig. 5. Effect of Sodium Chloride in the NP-OH Ternary Complex Using Polyplexes Formed with Various Concentrations of NaCl at a Charge Ratio (+/−) of 2/1 for PEI 600 on Size (A) and Transfection in PC-3 Cells (B)

Each value represents the mean±S.D. (n=4). $^{*}p<0.05$ and $^{**}p<0.01$, compared with the ternary complex formed in water. Comparison of cytotoxicity in PC-3 cells 48 h after transfection with the ternary complex formed in 50 mM NaCl (Fig. 5B) (C). Each column represents the mean±S.D. (n=4).

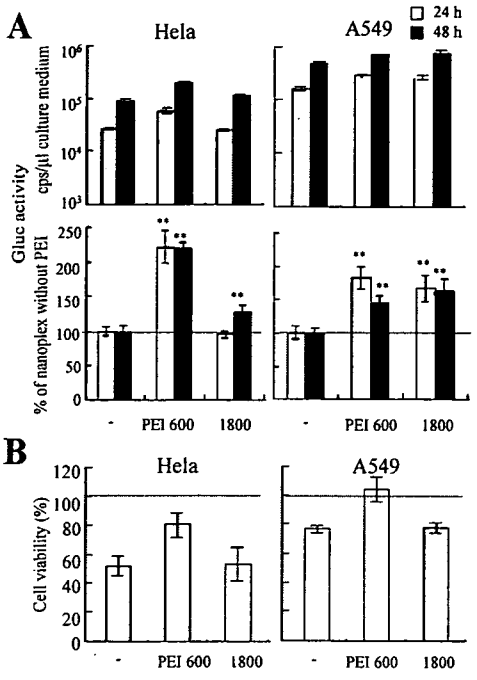

Fig. 6. Comparison of Transfection Levels (A) and Cytotoxicity (B) in Hela and A549 Cells by Ternary Complex 48 h after Transfection

Using polyplexes formed in a 50 mM NaCl solution at charge ratios (+/−) of 2/1 for PEI 600 and 1/1 for PEI 1800, the ternary complex was formed at a charge ratio (+/−) of 3/1. ** $p<0.01$, compared with the nanoplex formed in water. Each column represents the mean±S.D. ($n=4$).

tion was comparable to those for lipofectamine 2000 and lipofectamine LTX. Therefore, we decided to use 50 mM NaCl when forming nanoplexes as an optimal concentration of NaCl.

Cytotoxicity after Transfection of Ternary Complexes Next, we examined the cytotoxicity of the ternary complexes 48 h after transfection. We compared the cytotoxicity of the ternary complex, the lipofectamine 2000 lipoplex, or the lipofectamine LTX lipoplex in PC-3 cells. The lipofectamine 2000 and lipofectamine LTX lipoplexes exhibited significant toxicity (about 30% cell viability) (Fig. 5C). In contrast, ternary complexes did not actually exhibit cytotoxicity (80% cell viability). These findings indicated that PEI 600 could increase the transfection efficiency of NP-OH without cytotoxicity.

Comparison of Transfection Activity and Cytotoxicity in Hela and A549 Cells Finally, we investigated the transfection efficiency and cytotoxicity of PEI 600 and 1800 ternary complexes in other cells. In Hela and A549 cells, PEI 600 or 1800 combined with NP-OH, increased transfection 1.5-2-fold compared to the nanoplex alone (Fig. 6A). The cytotoxicity of the PEI 600 ternary complex was decreased compared with that of the nanoplex and PEI 1800 ternary complex (Fig. 6B). A lower molecular weight PEI was more effective in increasing transfection activity by NP-OH in Hela and A549 cells as well as PC-3 cells. These findings suggested that the combination of NP-OH and PEI 600 has great potential for efficient DNA transfection with low cytotoxicity.

DISCUSSION

In this study, we investigated the potential synergism of a PEI and NP-OH for the transfection of DNA into PC-3, Hela, and A549 cells, and demonstrated that NP-OH ternary complexes made using a low-molecular weigh PEI had higher levels of transfection efficiency than nanoplexes although the PEI polyplex alone did not exhibit effective gene transfection.

The size of a nanoplex is known to affect its transfection efficiency.[18—20] Increased transfection activity was observed when the NP-OH ternary complex was formed at concentrations of NaCl above 50 mM, even though the size was not significantly different with that formed in water (Figs. 5A, B). We previously reported that a marked dissociation of DNA from NP-OH nanoplexes was observed at low pH when the nanoplex of DNA was formed in NaCl solution.[16] Since the presence of NaCl did not increase significantly the size of the NP-OH ternary complex, the NaCl solution might influence the extent to which DNA dissociates from the NP-OH/PEI ternary complex. The presence of NaCl in forming ternary complex can weaken the association with DNA by neutralization of cationic charge on PEI or on the surface of NP-OH. The reason for the high transfection efficiency of the ternary complexes produced in the NaCl solution may be their instability in the endosome, resulting in the release of DNA from ternary complexes and the translocation of DNA into the cytoplasm.

The mechanistic pathway for gene transfection includes the compaction of the extended pDNA chain, known as DNA condensation.[21] Multivalent cations such as polyamines (spermidine, spermine), PEI and peptides (poly-L-lysine) are known to provoke the condensation of DNA to nanoparticles.[22,23] Regarding pDNA compaction with PEI, it has been reported that PEI 25K could form small polyplexes (100—250 nm) with pDNA, but PEI 2000 could not (greater than 3 μm),[15] indicating that PEIs with a large molecular weight could compact pDNA. PEIs of more than 11900 in molecular weight induced high gene transfection.[8] Therefore, the PEI used in this study could neither compact pDNA nor deliver pDNA into cells. The PEI of NP-OH ternary complex may act simultaneously in the release of DNA from endosomes, thus enhancing gene transfer. This finding corresponded to reports that the combination of Dosper liposome plus PEI 700 or 2000 caused the most effective transfection synergism.[13—15] With the combination of Dosper liposome and PEI 700, the PEI of the lipopolyplex had no effect on DNA condensation or the complex's size.[13,15] The PEI polyplex could protect the pDNA from degradation, or the transport of the PEI polyplex to the nucleus could be more effective than that of naked pDNA. PEI has the ability to more DNA into the nucleus.[10] These properties may be more effective with the small molecular PEIs.

When a lipopolyplex with effective transfection activity was formed at charge ratios (+/−) of 2.5/1 for PEI 2000 and 7.5/1 for Dosper liposome in a 150 mM NaCl solution, it was about 1500—3000 nm in size.[15] When a ternary complex was formed at charge ratios (+/−) of 2/1 for PEI 600 and 3/1 for NP-OH in a 50 mM NaCl solution, it was about 1000—1500 nm in size (Fig. 5A). These findings indicated that the ternary complex was smaller in size and in the

amount of cationic charge used in transfection than the lipopolyplex. The combination of NP-OH and PEI 600 might be valuable for pDNA transfection.

We used the WST-8 assay for the cytotoxicity assessment. In PC-3, Hela, and A549 cells, only low toxicity was found on transfection with the PEI600 ternary complex (about 80—100% cell viability) (Figs. 5C, 6B). The higher molecular weight of PEIs (PEI 1800) increased cytotoxicity when combined with NP-OH (Fig. 6B). PEIs with low-molecular weight are reported to be less cytotoxic than those with high-molecular weight.[8] These findings may explain the rather low toxicity obtained with the PEI 600 ternary complex. For the development of transfection reagents with low cytotoxicity, it is neccessary to have sufficient transfection efficiency with as little cationic lipid as possible. Increasing the charge ratio (+/−) of cationic nanoparticles/pDNA increased not only transfection efficiency but also cytotoxicity by increasing the lipid concentration. Combining NP-OH with PEI 600 allows the use of a smaller amount of NP-OH to obtain sufficient transfection efficiency without an increase of cytotoxicity.

In this study, we demonstrated that the combination of NP-OH and a PEI of low-molecular weight could serve as an efficient vector for DNA transfer, being comparable with commercial reagents. The combination of a PEI polymer and lipid-based nanoparticles is a potential non-viral DNA vector for gene delivery.

Acknowlegements This project was supported in part by a Grant-in-Aid for Scientific Research from the Ministry of Education, Culture, Sports, Science and Technology of Japan.

REFERENCES

1) Dass C. R., Burton M. A., *J. Pharm. Pharmacol.*, **51**, 755—770 (1999).
2) Hasegawa S., Hirashima N., Nakanishi M., *Bioorg. Med. Chem. Lett.*, **12**, 1299—1302 (2002).
3) Nakanishi M., *Curr. Med. Chem.*, **10**, 1289—1296 (2003).
4) Godbey W. T., Wu K. K., Mikos A. G., *J. Control Release*, **60**, 149—160 (1999).
5) Boussif O., Lezoualc'h F., Zanta M. A., Mergny M. D., Scherman D., Demeneix B., Behr J. P., *Proc. Natl. Acad. Sci. U.S.A.*, **92**, 7297—7301 (1995).
6) Kichler A., Leborgne C., Coeytaux E., Danos O., *J. Gene Med.*, **3**, 135—144 (2001).
7) Godbey W. T., Wu K. K., Mikos A. G., *J. Biomed. Mater. Res.*, **45**, 268—275 (1999).
8) Fischer D., Bieber T., Li Y., Elsasser H. P., Kissel T., *Pharm. Res.*, **16**, 1273—1279 (1999).
9) Abdallah B., Hassan A., Benoist C., Goula D., Behr J. P., Demeneix B. A., *Hum. Gene Ther.*, **7**, 1947—1954 (1996).
10) Pollard H., Remy J. S., Loussouarn G., Demolombe S., Behr J. P., Escande D., *J. Biol. Chem.*, **273**, 7507—7511 (1998).
11) Boletta A., Benigni A., Lutz J., Remuzzi G., Soria M. R., Monaco L., *Hum. Gene Ther.*, **8**, 1243—1251 (1997).
12) Goula D., Benoist C., Mantero S., Merlo G., Levi G., Demeneix B. A., *Gene Ther.*, **5**, 1291—1295 (1998).
13) Lampela P., Soininen P., Urtti A., Mannisto P. T., Raasmaja A., *Int. J. Pharm.*, **270**, 175—184 (2004).
14) Lampela P., Raisanen J., Mannisto P. T., Yla-Herttuala S., Raasmaja A., *J. Gene Med.*, **4**, 205—214 (2002).
15) Lampela P., Elomaa M., Ruponen M., Urtti A., Mannisto P. T., Raasmaja A., *J. Control Release*, **88**, 173—183 (2003).
16) Hattori Y., Kubo H., Higashiyama K., Maitani Y., *J. Biomed. Nanotech.*, **1**, 176—184 (2005).
17) Hattori Y., Ding W., Maitani Y., *J. Control Release*, **120**, 122—130 (2007).
18) Almofti M. R., Harashima H., Shinohara Y., Almofti A., Li W., Kiwada H., *Mol. Membr. Biol.*, **20**, 35—43 (2003).
19) Turek J., Dubertret C., Jaslin G., Antonakis K., Scherman D., Pitard B., *J. Gene Med.*, **2**, 32—40 (2000).
20) Zaric V., Weltin D., Erbacher P., Remy J. S., Behr J. P., Stephan D., *J. Gene Med.*, **6**, 176—184 (2004).
21) Bloomfield V. A., *Curr. Opin. Struct. Biol.*, **6**, 334—341 (1996).
22) De Smedt S. C., Demeester J., Hennink W. E., *Pharm. Res.*, **17**, 113—126 (2000).
23) Vijayanathan V., Thomas T., Thomas T. J., *Biochemistry*, **41**, 14085—14094 (2002).